AWARD NUMBER: W81XWH-20-1-0577

TITLE: The Influence of Adipogenic Progenitors and Duffy-Null Phenotype on the Normal Breast and Breast Cancer Biology of Women of African Descent

PRINCIPAL INVESTIGATOR: Harikrishna Nakshatri

CONTRACTING ORGANIZATION: Indiana University

REPORT DATE: JULY 2021

TYPE OF REPORT: Annual Report

PREPARED FOR: U.S. Army Medical Research and Development Command
Fort Detrick, Maryland 21702-5012

REPORT DOCUMENTATION PAGE

Form Approved
OMB No. 0704-0188

1. REPORT DATE
JULY 2021

2. REPORT TYPE
Annual

3. DATES COVERED
07/01/2020 – 06/30/2021

4. TITLE AND SUBTITLE
The Influence of Adipogenic Progenitors and Duffy-Null Phenotype on the Normal Breast and Breast Cancer Biology of Women of African Descent

5a. CONTRACT NUMBER

5b. GRANT NUMBER
W81XWH-20-1-0577

5c. PROGRAM ELEMENT NUMBER

5d. PROJECT NUMBER

5e. TASK NUMBER

5f. WORK UNIT NUMBER

6. AUTHOR(S)

Harikrishna Nakshatri

E-Mail: hnakshat@iupui.edu

7. PERFORMING ORGANIZATION NAME(S) AND ADDRESS(ES)

Indiana University School of Medicine, Indianapolis, IN 46202

8. PERFORMING ORGANIZATION REPORT NUMBER

9. SPONSORING / MONITORING AGENCY NAME(S) AND ADDRESS(ES)

U.S. Army Medical Research and Development Command
Fort Detrick, Maryland 21702-5012

10. SPONSOR/MONITOR'S ACRONYM(S)

11. SPONSOR/MONITOR'S REPORT NUMBER(S)

12. DISTRIBUTION / AVAILABILITY STATEMENT

Approved for Public Release; Distribution Unlimited

13. SUPPLEMENTARY NOTES

14. ABSTRACT

Breast cancer is African American women tend to be highly aggressive and metastatic compared to breast cancers in Caucasian women. Within African American women, those who carry inherited duffy null or heterozygous alleles show even worse outcome from breast cancer. We had previously demonstrated elevated number of PROCR+/ZEB1+/PDGFRA+ (PZP) cells in the normal breast of African American women and breast epithelial cells in duffy null/heterozygous carriers have elevated activity of cMET oncogene. In this year report, we have characterized PZP cells further and found that interaction between PZP cells and breast epithelial cells leads to elevated expression of interleukin 6, which could lead to changes in the tumor microenvironment that enhance metastasis. Similar to ZEB1+ cells, normal breast tissues of African American women express higher levels of PROCR and PDGFRA. With respect to duffy phenotype, we have generated breast epithelial cell lines from duffy heterozygous women and transformed these cell lines with HRASG12V and mutant p53. These cell lines are being characterized for growth and metastasis in vivo.

15. SUBJECT TERMS

NONE LISTED

16. SECURITY CLASSIFICATION OF:			**17. LIMITATION OF ABSTRACT**	**18. NUMBER OF PAGES**	**19a. NAME OF RESPONSIBLE PERSON**
a. REPORT	**b. ABSTRACT**	**c. THIS PAGE**			USAMRMC
Unclassified	Unclassified	Unclassified	Unclassified	34	**19b. TELEPHONE NUMBER** *(include area code)*

TABLE OF CONTENTS

Introduction: African American (AA) women suffer higher mortality from triple negative breast cancer (TNBC) than Caucasian women. By contrast, breast cancer in Hispanic and Native American women is less prevalent and these women have a better outcome. Whether worst outcome in AA women is due to an increased incidence of TNBC or unique biological factors that promote aggressive biology is an important but unresolved challenge in cancer disparity research. Recent studies have also demonstrated that duffy heterozygous/null phenotype, which is most commonly inherited in people of sub-Saharan ancestry, is associated with aggressive breast cancer biology in African American women, which provided first hint to the impact of genetic ancestry influencing the biology of breast cancer. We previously reported that the normal breasts in AA women are enriched for cells that express ZEB1, an epithelial to mesenchymal transition associated transcription factor. In in vitro studies, these cells also expressed PROCR and PDGFRalpha (PDGFRα). Therefore, we labelled these cells as PZP cells. One aim of the proposal is focused on further characterizing these cells. In our preliminary studies, we had observed that breast epithelial cells from duffy-heterozygous and duffy-null carriers have higher levels of activated cMET signaling. Since cMET pathway is associated with chemotherapy resistance and metastasis, the second aim is focused on testing the hypothesis that duffy-heterozygous and duffy-null phenotype confers aggressive metastatic property to breast cancer through cMET pathway.

Keywords: Breast cancer, PROCR, ZEB1, PDGFRalpha, Duffy, drug resistance, metastasis.

Accomplishments:

Specific Aim 1. To investigate the intrinsic and extrinsic effects of PZP cells enriched in AA women on tumorigenesis	**Cell lines and cohorts**	**Timeline Months**	**Current status**
Major Task 1. Trans-differentiating properties of PZP cells of the normal breast:			
Subtask 1 (6.1.2): Characterize PZP cells for trans-differentiation upon treatment with various ligands of PDGFR.	KTB40 and KTB42. Note that we have four other similar cell lines in stock but only two will be used (KTB32, KTB53, KTB55 and KTB59)	1-5	Work in progress
Subtask 2 (6.1.3): Determine how cancer cell-induced factors modulate trans-differentiation	Cancer cell lines MCF-7, T47-D, SK-BR-3, BT-474, HCC1937, MDA-MB-468, SUM149PT, HCC70, HCC1187, DU4475, BT-549, HS578T, MDA-MB-231 and MDA-MB-436. PZP lines KTB40 and KTB42	2-12	Work in progress
Milestone Achieved: demonstrated that PZP cells upon trans-differentiation into fibroblasts, adipocytes or osteoblasts alter tumor progression			
Major Task 2 (6.1.4): Determine whether cancer cell-derived factors cause PDGFRα isoform switching or receptor dimerization to enhance differentiation to fibroblasts			
Subtask 3: Determine the effects of conditioned media from cell lines on PDGFRα isoforms in PZP cells.	Conditioned media from cancer cell lines listed in subtask 2	13-15	Yet to be initiated
Milestones achieved: Conditioned media from select cell lines block the generation of decoy PDGFRα receptor.			
Major Task 3 (6.1.5). The effects of trans-differentiated PZP cells on invasive and drug sensitivity of various breast cancer cell lines:			
Subtask 4: Generate GFP labeled PZP cells and trans-differentiate cells into fibroblasts, adipocytes, or osteoblasts	Parental and transdifferentiated KTB40 and KTB42	10-14	GFP+ cells have been generated
Subtask 5: Perform co-culture experiments to determine the influence of various trans-differentiated PZP cells on cancer cell invasion	Cancer cell lines described in subtask 2 plus oncogene transformed breast epithelial cell lines from two each of Caucasian, Hispanic and African American women, parental	14-20	Partially completed. Have identified IL-6 as a factor secreted at a higher levels when PZP and breast epithelial cells are in contact.

	and transdifferentiated KTB40 and KTB42		
Subtask 6: Perform drug sensitivity studies of co-cultured cells	Cell lines described in subtask 5	20-24	
Milestone achieved: PZP cells, depending on type of trans-differentiation altered sensitivity of cancer cells to chemotherapy and influenced their invasive properties			
Major Task 4 (6.1.6). The effects of trans-differentiated PZP cells on growth and metastatic properties of breast cancer cells *in vivo*:			
Subtask 7: Determine the effects of trans-differentiated PZP cells on growth and metastasis of cancer cells	Cell line: One transformed cell line derived from epithelial cells of Caucasian and another from African American women, MCF-7 and MDA-MB-468 cell line. Parental and transdifferentiated KTB40 or KTB42 Animal: NSG mice. Cohort size: 336 (4 tumor lines with 7 types of PZP cells, 12 animals per group	20-28	Cancer cell lines expressing tomato-red luciferase have been created and work will begin soon.
Milestone(s) Achieved: Demonstrated the role of PZP cells in growth and metastasis of tumor cells in vivo.			
Major Task 5 (6.1.7): Determine whether the PDGFRα inhibitor nilotinib can reduce PZP cells activity and increase chemosensitivity			
Subtask 8: Implant tumor cells with PZP cells and determine sensitivity of tumors to nilotinib ± paclitaxel.	Cell lines: A transformed cell line derived from African American women plus one PZP cell line. Mice: NSG Cohort: 96 (48 animals without PZP cells and 48 with PZP cells. Four treatment groups, 12 per group. Control, nilotinib, paclitaxel and both drugs.	22-32	Yet to be initiated
Milestones Achieved: Nilotinb increases sensitivity of tumors to chemotherapeutic drug paclitaxel			
Major Task 6 (6.1.8): Intrinsic tumorigenic properties of PZP cells:			
Subtask 9: Transform parental PZP or PZP cells trans-differentiated into epithelial cells and determine their tumorigenic properties	Cell lines: Three PZP cell lines transformed using two different oncogenes-total six cell lines. Mice: NSG. Cohort: Six cell lines, 12 animals per cell line. Total 72 animals.	20-28	Work is partially done. PZP cells generate metaplastic carcinoma when transformed with HRASG12V plus SV40 T/t antigens.
Milestone achieved: Epithelial trans-differentiated PZP cells generate tumors with distinct characteristics			
Specific Aim 2. To investigate the role of hyperactive c-MET signaling in breast tumorigenesis under the duffy-null background			
Major Task 7 (6.2.2). *In vitro* characterization of immortalized and transformed duffy-wild type, duffy-heterozygous and duffy-null breast epithelial cell lines:			
Subtask 10: Generate immortalized and transformed cell lines with duffy wild type, duffy-heterozygous and duffy-null background	Cell lines: Two each of duffy wild type, duffy-heterozygous and duffy-null immortalized cell lines; each transformed with two sets of oncogenes. 18 cell lines (six immortalized and 12 transformed)	1-12	Generated immortalized and transformed variants of one wild type and one duffy-heterozygous breast epithelial cells.

Subtask 11: Determine CCL2 and CXCL8 mediated signaling in all cell types by proteomics and RNA-seq	Cell lines described in subtask 10	12-24	Immortalized cell lines have been subjected to RTK array
Milestone achieved: Distinct CCL2 and CXCL8 signaling in duffy-heterozygous and duffy-null epithelial cells compared to duffy wild type cells.			
Major Task 8 (6.2.3): Stem cells properties of duffy-null/heterozygous cells			
Subtask 12: Determine tumor-initiating capacity of transformed duffy-wild type, duffy-heterozygous and duffy-null cell lines	Cell lines: two each of transformed cell lines in duffy-wild type, duffy-heterozygous and duffy-transformed background. Mice: NSG Cohort: 3 cell dilutions, 5 per dilution, 2 cell lines per category and three categories, Total 90 animals	24-28	Transformation has been achieved with $HRAS^{G12V}$ plus mutant p53. Wild type cells with $HRAS^{G12V}$ plus mutant p53 but not PIK3CAH1047R+ mutant p53 generated tumors in NSG mice.
Milestones achieved: Transformed cell lines under duffy-null background have higher tumor-initiating capacity.			
Major Task 9: The influence of duffy phenotype on drug sensitivity			
Subtask 13: Determine the sensitivity of immortalized and transformed cells to doxorubicin, paclitaxel, and cisplatin	Cell lines: two each of immortalized and transformed cell lines under duffy-wild types, duffy-heterozygous and duffy-null background	12-17	Yet to be initiated
Milestones achieved: Transformed cells under duffy-null and duffy-heterozygous background are resistant to chemotherapy.			
Major Task 10 (6.2.5). The ability of c-MET inhibitors to sensitize transformed duffy-null cells to chemotherapy:			
Subtask 14: Determine sensitivity of duffy wild type, duffy heterozygous, and duffy null immortalized and transformed cells to crizotinib or carbozantinib with and without chemotherapeutic drugs *in vitro*	Cell lines: same as described in subtask 13	13-20	Yet to be initiated
Major Task 11 (6.2.6). In vivo effects of duffy-null/heterozygous phenotype on tumorigenicity, metastasis and drug sensitivity			
Subtask 15: Measure tumor growth rate and lung metastasis of transformed duffy-wild type, duffy-heterozygous and duffy-null cell derived tumors	Cell lines: Transformed cell lines from each category but transformed by two different sets of oncogenes Mice: NSG Cohort: 12 transformed cell lines, 12 animals per cell line and 144 animals	20-26	Yet to be initiated
Subtask 16: Measure the effects of Crizotinib with and without chemotherapy on tumor growth and metastasis	Cell lines: One each of transformed cell line under duffy-wild type, duffy-heterozygous and duffy-null background. Mice: NSG mice. Cohort: 72 animals per cell line, each cell line in 6 groups (control, crizotinib, chemo-1, chemo-2, crizotinib plus chemo-1, crizotinib plus chemo-2.) Three cell lines. 216 animals	27-34	Yet to be initiated.
Milestone achieved: Duffy-heterozygous or duffy-null compared to duffy wild type transformed epithelial cells are more sensitive to crizotinib or carbozantinib ± chemotherapy both in vivo and in vitro			

Subtask 17: Write Manuscript based on results of aims 1 and 2.	12-16 and 33-36	

Specific aims:

<u>Aim 1:</u> To investigate the intrinsic and extrinsic effects of PZP cells enriched in AA women on tumorigenesis.

PZP cells are enriched in the normal breasts of AA women compared with CA women: We generated a tissue microarray (TMA) comprising healthy breast tissues from 50 African American (AA), 150 white (Caucasian) and 50 Latina women and analyzed the TMA for protein levels of PROCR, ZEB1 and PDGFRα by immunohistochemistry (IHC). Statistical analyses of IHC staining of PROCR, ZEB1, and PDGFRα are shown in **Tables 1-3.**

Table 1. Compare H-score and Positivity between race in all patients within Normal tissue for PROCR

	race				
variable label	COLUMN_OVERALL	African American N=31	Caucasian N=129	Latino N=33	P-value
Positivity	0.17 (0.04, 0.55)	0.30 (0.06, 0.55)	0.15 (0.04, 0.41)	0.17 (0.04, 0.39)	<.0001
H-Score	27.97 (5.45, 127.65)	56.41 (10.46, 127.65)	24.37 (6.68, 83.50)	26.06 (5.45, 72.30)	<.0001

Table 2. Compare H-score and Positivity between race in all patients within Normal tissue for ZEB1

	race				
variable label	COLUMN_OVERALL	African American N=33	Caucasian N=144	Latino N=28	P-value
Positivity	0.01 (0.00, 0.24)	0.01 (0.00, 0.10)	0.01 (0.00, 0.12)	0.02 (0.00, 0.24)	0.0380
H-Score	1.62 (0.15, 30.72)	2.21 (0.24, 16.47)	1.46 (0.15, 19.76)	2.75 (0.40, 30.72)	0.0076

Table 3. Compare H-score and Positivity between race in all patients within Normal tissue for PDGFRα

	race				
variable label	COLUMN_OVERALL	African American N=35	Caucasian N=154	Latino N=18	P-value
Positivity	0.10 (0.01, 0.75)	0.28 (0.03, 0.75)	0.09 (0.01, 0.73)	0.09 (0.02, 0.56)	<.0001
H-Score	16.30 (1.43, 110.23)	36.96 (6.25, 110.23)	14.27 (1.43, 88.61)	12.61 (2.69, 73.08)	<.0001

Note: Values expressed as median (min, max)

Note: P-value comparisons across race categories are based on Wilcoxon (Normal Approximation)

Consistent with our previous report regarding ZEB1 [1], breast tissues of AA women displayed higher ZEB1 H-score compared to Caucasian women. Surprisingly, normal breast tissues of Latina also demonstrated higher H-score for ZEB1. With respect to PROCR and PDGFRα, normal breast tissues of only AA women contained significantly higher levels of expression (both positivity and H-Score) compared to Caucasian and Latina. Thus, enrichment of PZP cells is unique to AA women.

Characterization of PROCR+/ZEB1+/PDGFRα (PZP cells) derived from healthy breast tissues of AA women. We have created six immortalized cell lines from AA (KTB40, KTB42, KTB32, KTB53, KTB57, and KTB59) by overexpressing human telomerase gene (hTERT) in primary cells isolated and propagated from core breast biopsies of healthy women. Self-reported ethnicity does not always match with genome-driven ethnicity as determined by ancestry mapping. To ensure that the above KTB cell lines are from AA women based on genetic ancestry, all samples were subjected to highly discriminative ancestry informative 41-SNP (single nucleotide polymorphism) genomic analyses [2]. As shown in **Fig. 1A**, self-reported African American women had inherited >50% of African ancestry markers. In the mouse mammary gland, PROCR+/EpCAM- cells are suggested to function as multi-potent stem cells [3]. We subjected these KTB cell lines to flow cytometry using PROCR (CD201) and EpCAM markers, and all KTB cell lines from AA women were predominantly PROCR+/EpCAM- **(Fig. 1B and 1C)**. These cells are enriched for the expression of stemness- related transcription factor *ZEB1* and have enhanced Wnt pathway activity compared to PROCR±/EpCAM+ cells [4]. To further characterize

PROCR+/EpCAM- cells for stem-cell activity, we compared these immortalized variants with the immortalized PROCR±/EpCAM+ luminal/basal cells from CA, and AA women. PROCR+/EpCAM- cell lines expressed significantly higher levels of *ZEB1* compared to PROCR±/EpCAM+ cell lines **(Fig. 1D).** Morphologically, PROCR+/EpCAM- cell lines showed features of epithelial to mesenchymal transition (EMT) **(Fig. 1E)**.

PROCR+/ZEB1+ cells show similarity to adipogenic progenitors that trans-differentiate into epithelial cells: A recent study described PDGFRα+ stromal cells as adipogenic progenitors of the mammary gland that trans-differentiate into epithelial cells and migrate into the duct when stimulated by PDGF-C [5]. Interestingly, these cells also expressed PROCR [5]. We examined whether these PROCR+/ZEB1+ cells express PDGFRα. Indeed, >70% of cells were PDGFRα+ **(Fig. 2A and 2B).** Confluent PROCR+/EpCAM+ cells underwent adipogenic differentiation when supplemented with appropriate media further suggesting pluripotent nature of these cells **(Fig. 2C)**. Thus, PROCR+/ZEB1+/PDGFRα+ (named PZP) cells enriched in the breasts of AA women could correspond to multipotent cells that can trans-differentiate into epithelial cells based on environmental ques.

PZP cells show the lobular fibroblasts phenotype: In the human breast tissue, loose connective tissue is unique for the terminal duct lobular units (TDLUs), which drain into the interlobular ducts, which in turn are embedded in a more dense connective tissue [6]. CD105^{high} TDLU-resident lobular fibroblasts display the properties different from interlobular fibroblasts [7]. While the CD105^{high} lobular fibroblasts resemble mesenchymal stem cells (MSCs) both by phenotype and function, CD26^{high} interlobular cells remain fibroblast restricted [7]. CD105^{high}/CD26^{low} and CD105^{low}/CD26^{high} lineages are considered to represent lobular and interlobular human breast fibroblastic cells (HBFCs), respectively [8]. To further characterize the immortalized PZP cell lines, we examined the CD105 and CD26 staining pattern. PZP cells were enriched for CD105^{high}/CD26^{low} population with inter-individual variability in the ratio between

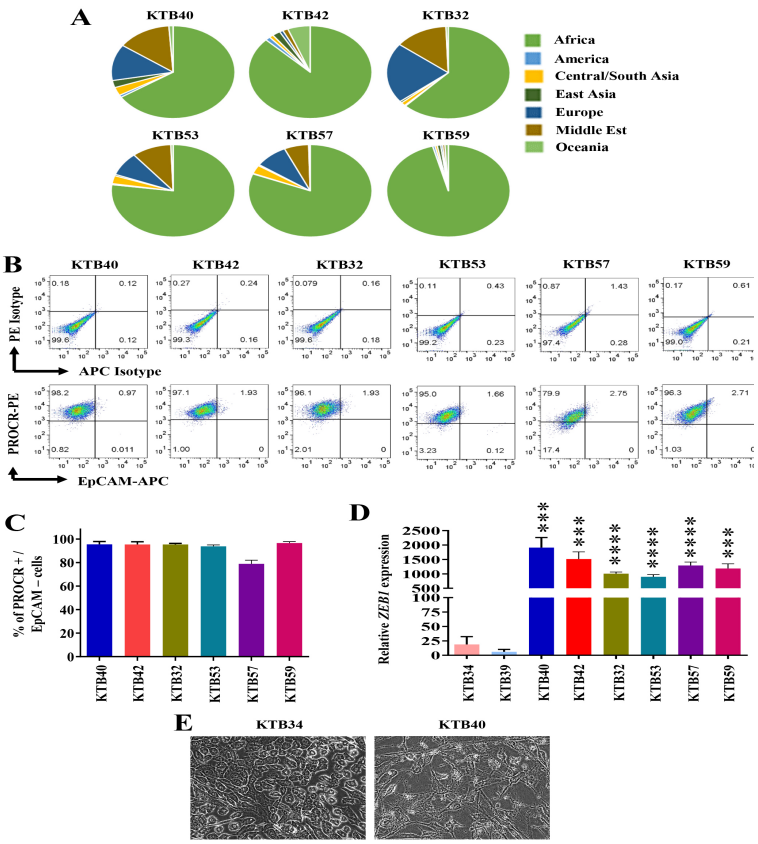

Fig. 1: (A) Genetic ancestry mapping of African American (KTB40, KTB42, KTB32, KTB53, KTB57, KTB59) women based on the genotype analysis using a panel of 41-SNP along with a Bayesian clustering method. (B) PROCR+/EpCAM- cells are enriched in the normal breast of AA women. (C) Quantitation of PROCR+/EpCAM- cells. (D) *ZEB1* expression levels in various PROCR+/EpCAM- cell lines compared to EpCAM+ cells. (E) Phase contrast images representing the epithelial morphology of human telomerase gene (hTERT) immortalized breast epithelial cells (KTB34) and features of epithelial to mesenchymal transition (KTB40).

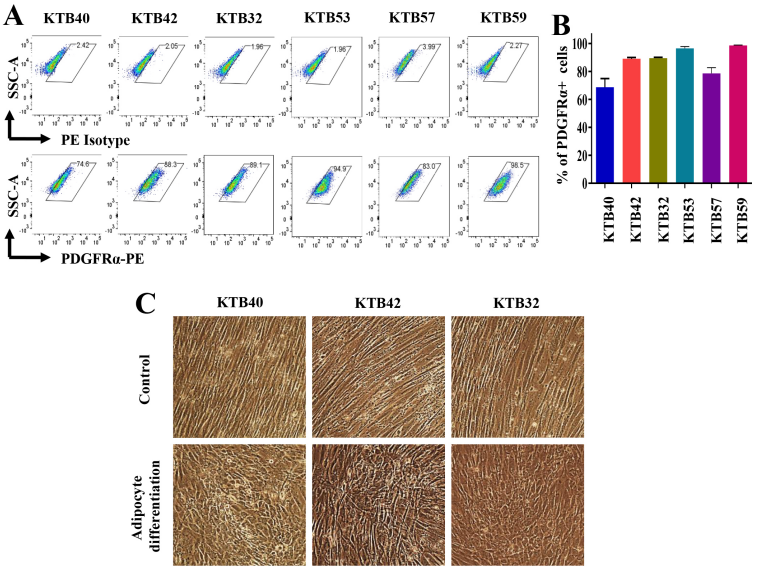

Fig. 2: (A) PROCR+/ZEB1+ cells express PDGFRα. Flow cytometry shows PDGFα cells. (B) Quantitation of PDGFα cells. (C) PZP cells undergo adipogenic differentiation under appropriate growth condition. Neural lipids stain red upon Oil Red-O staining.

CD105^{high}/CD26^{-} and CD105^{high}/CD26^{low} **(Fig. 3A-3C)**, which suggested that PZP cells are derived from lobular origin of human breast tissue.

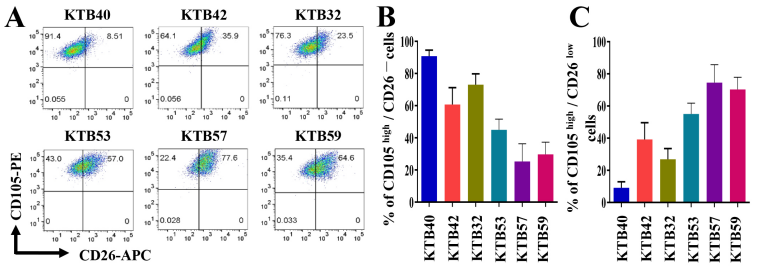

Fig. 3: (A) PZP Cell lines were stained with CD105 and CD26 antibodies to identify the lobular and interlobular origin of human breast fibroblastic cells. (B and C) Quantification of CD105^{high}/CD26^{-} and CD105 ^{high}/CD26 ^{low} population of cells.

Phenotypic characterization of PZP cells; are these subepithelial mesenchymal cells?

CD90^{-}/CD73^{+} and CD73^{+}/CD90^{+} are described as rare endogenous pluripotent somatic stem cells and potential mesenchymal stem cells, respectively [9]. PZP cells showed CD90^{-}/CD73^{+} and CD73^{+}/CD90^{+} populations, with remarkable inter-individual variability in the ratio between CD90^{-}/CD73^{+}, CD90^{low}/CD73^{+} and CD90^{high}/CD73^{+} **(Fig. 4A-4D)**. CD44 and CD24 are the "original" markers used to characterize cancer stem cells (CSCs) in breast cancer [10]. However, PZP cells displayed CD44^{+}/CD24^{-} population, which indicated the characteristic of stem/basal cells **(Fig. 4E and F)**. CD10 marker is used to isolate myoepithelial cells, although a recent study showed CD10 positivity of cancer associated fibroblasts [11, 12]. PZP cells showed CD10^{+} phenotype **(Fig. 4G and H)**. CD49f^{high}/EpCAM^{low}, CD49f^{high}/EpCAM^{medium}, and CD49f^{low}/EpCAM^{high} cells are described as breast stem, luminal progenitor, and mature/differentiated cells, respectively [13]. None of the PZP cell lines were positive for CD49f and EpCAM **(Fig. 4I)**.

Transgelin (TAGLN) is known to be a specific marker of smooth muscle differentiation and highly expressed in the myoepithelial cells and fibroblastic cells of benign breast tissue [14]. Normal luminal cells are predominantly negative or display weak expression [14, 15]. A population of subepithelial cells that lines the entire villus-crypt axis of intestine express high levels of PDGFRα, DLL1, F3, and EGF-family ligand Neuregulin 1 (NRG1) [16]. In addition, NRG1 is also expressed in mesenchymal cells adjacent to the proliferative crypts [16]. In order to identify the major cell types within PZP cells, we examined the expression of TAGLN, DLL1, F3 and NRG1 in PZP cell lines (KTB32, KTB40, KTB42), luminal epithelial cells (luminal progenitor; KTB34, KTB39), and co-culture of PZP and epithelial cell lines (50% of each cell line). We observed abundant TAGLN expression in PZP cells, while epithelial cells expressed at low level. Interestingly, the expression of TAGLN was synergistically increased under co-culture condition **(Fig. 5A, Table 4)**. We found a low level of DLL1, F3, and NRG1 expression in PZP cell lines except high

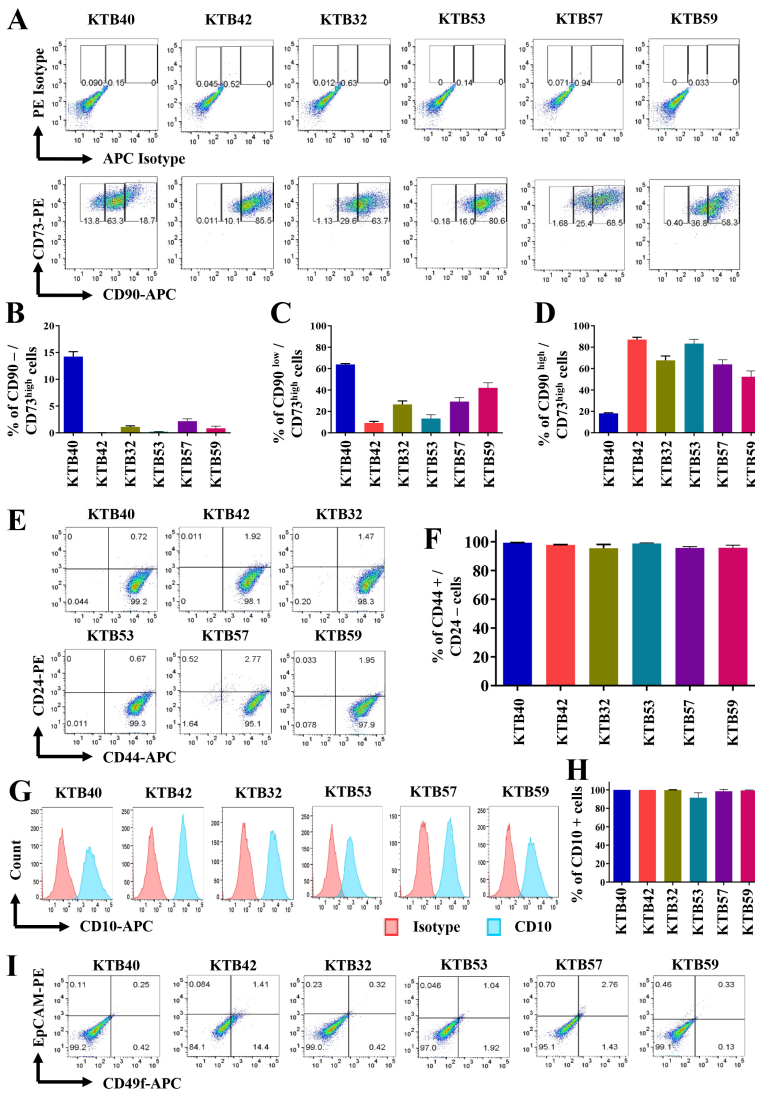

Fig. 4: (A) PZP Cell lines were stained with CD90 and CD73 antibodies to identify the rare endogenous pluripotent somatic stem cells and potential mesenchymal stem cells. (B, C and D) Quantification of CD90^{-} /CD73^{high}, CD90^{low}/CD73^{high}, CD90^{high}/CD73^{high} population of cells. (E) PZP Cell lines were stained with CD44 and CD24 antibodies to identify the cancer stem cells. (F) Quantification of CD44^{+}/CD24^{-} population. (G) PZP Cell lines were stained with CD10 antibody to identify the myoepithelial cells. (H) Quantification of CD10^{+} population. (I) PZP Cell lines were stained with CD49f and EpCAM antibodies to demonstrate the breast stem, luminal progenitor, and mature/differentiated cells.

level of NRG1 in KTB42. DLL1, F3 and NRG1 are expressed predominantly in epithelial cell lines. In co-cultured cells, expression of DLL1 and F3 was additive depending on the cell type **(Fig. 5B-D, Table 4)**. Taken together, these results indicate that PZP cells correspond to multi-lineage cells that interacts with epithelial cells to alter gene expression in a reciprocal manner. However, these cells are unlikely to function similar to subepithelial mesenchymal cells described in the intestine [16].

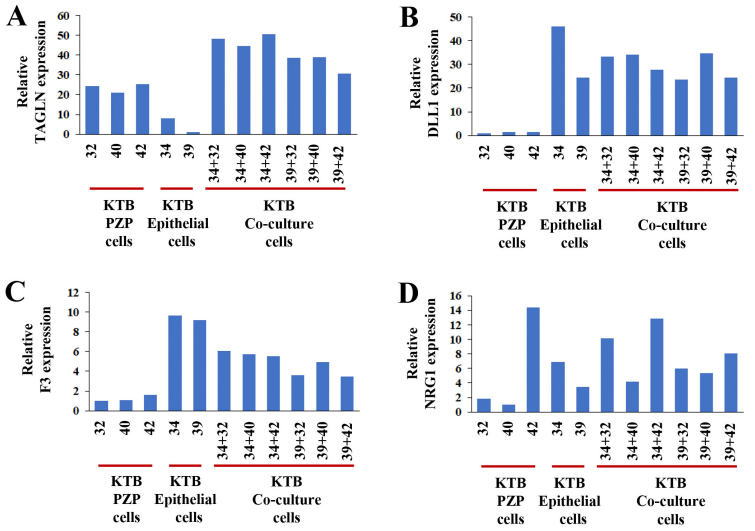

Fig. 5: Expression of TAGLN (A), DLL1 (B), F3 (C), and NRG1 (D) in PZP cell lines (KTB32, KTB40, KTB42), epithelial cells (luminal progenitor; KTB34, KTB39), and co-culture of PZP and epithelial cells cell lines.

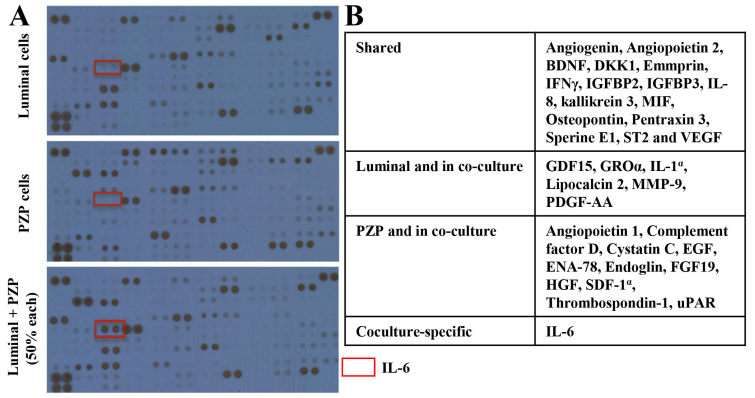

Fig. 6: (A and B) Only luminal and PZP cells co-culture releases IL-6. R&D systems cytokine/chemokine array was used to identify secreted factors by luminal and PZP cells either alone or together (50% each).

Establishing the cell-intrinsic and extrinsic effects of PZP cells on tumorigenesis.

We had proposed that PROCR+/ZEB1+ cells of the breast are the source of different stromal cells within breast cancer. Ligand type (PDGF-A versus PDGF-B, C and D) and ligand abundance (PDGF-A) for PDGFRα, receptor dimerization (α/α, β/β, and α/β), and cancer-derived signals that alter miR-206, RUNX1 or PDGFRα isoform expression in these cells would determine the composition of the breast tumor microenvironment. For example, trans-differentiation into fibroblast lineage may be responsible for increased levels of cancer-associated fibroblasts (CAFs), whereas trans-differentiation into osteogenic lineage may be responsible for microcalcification of tumors. Increased levels of CAFs as well as microcalcification are associated with worst outcome in breast cancer [17, 18]. To obtain potential insight into signaling pathway alterations in epithelial and PZP cells as a consequence of their cross-talk, we performed cytokine/chemokine profiling of factors secreted by an immortalized luminal epithelial cell line, a PZP cell line and both co-cultured together (50% of each cell line) for ~12 hours. While luminal epithelial cell line expressed several ligands such as PDGF-AA and osteopontin, which can affect trans-differentiation of PZP cells, PZP cells expressed factors such as EGF, HGF and SDF-1α, which can signal in luminal cells (**Fig. 6A and B**). Interestingly, IL-6 is produced only under co-culture condition. We further confirmed the IL-6 production under co-culture condition at mRNA level by qRT-PCR **(Fig. 7A, Table 4)**. We suspect PZP cells produce IL-6 in response to interaction with luminal cells as luminal cells secreted IL-1α, which we have previously shown to induce IL-6 in stromal cells [19]. There appears to be specificity in cytokine production under co-culture conditions as we did not observe the production of IL-8 under co-culture condition of PZP and epithelial cells **(Fig. 7B, Table 4)**. Thus, PZP cell-luminal cell interaction can lead to trans-differentiation of PZP cells and production of pro-invasive and pro-metastatic factor IL-6. Abundance of PZP cells under normal state in AA compared to CA women enables tumors in AA women to readily engage with PZP cells to build an aggressive tumor microenvironment. Restricting the activity of PZP cells through either PDGFRα inhibition or by promoting trans-differentiation into epithelial cells may dampen the tumor microenvironment and restrict tumor growth.

A

Coculture-specific effect	Gene expression
Synergistic	IL-6, TAGLN
Additive	WISP1, TNC, DLL1, CSF1, SPP1
Inhibition	IL-33
No effect	IL-4, IL-8, CMTM6, MIF, NRG1, F3, MFGE8, POSTN

B

Gene expression	PZP cells	Epithelial cells	Co-culture
IL-6	+ +	+ +	+ + + + + +
TAGLN	+ + + +	+ +	+ + + + + +
WISP1	+ + + +	+	+ + + +
TNC	+ +	+ + + +	+ + + +
DLL1	+	+ + + +	+ + + +
CSF1	+ + + +	+ +	+ + + +
SPP1	+ + + +	+ +	+ + + +
IL-33	+ +	+ +	+
IL-4	+ +	+ + + +	+ + +
IL-8	+ +	+ + + +	+ + +
CMTM6	+ +	+ + + +	+ + +
MIF	+ +	+ + + +	+ +
NRG1	+ +	+ + + +	+ + +
F3	+ +	+ + + +	+ + +
MFGE8	+ + + +	+ +	+ + +
POSTN	+ + + +	+ +	+ + +

Table 4: (A) Co-culture effect on gene expression. (B) Representative expression of genes in PZP cell lines (KTB32, KTB40, KTB42), luminal progenitor (epithelial cells; KTB34, KTB39), and co-culture of PZP and luminal progenitor cell lines.

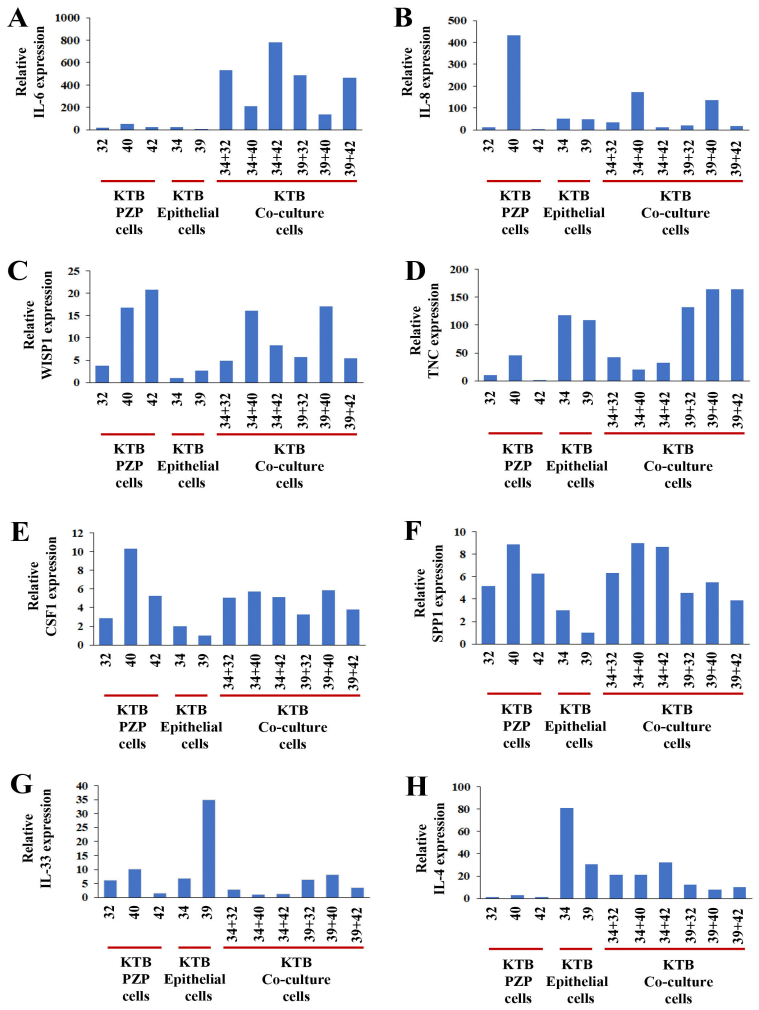

Fig. 7: Effect of co-culture of PZP and luminal progenitor cell lines on expression of genes. Expression of IL-6 (A), IL-8 (B), WISP1 (C), TNC (D), CSF1 (E), SPP1 (F), IL-33 (G), and IL-4 (H) in PZP cell lines (KTB32, KTB40, KTB42), luminal progenitor (epithelial cells; KTB34, KTB39), and co-culture of PZP and luminal progenitor cell lines.

pathway protein 1 (WISP1) expression affects the clinical prognosis through associations with macrophage M2 polarization, and immune cell infiltration in pan-cancer and helps to maintain CSC properties in glioblastoma [20, 21]. PZP cell lines displayed higher expression of WISP1, epithelial cell lines showed low expression, while additive expression was observed under co-culture except KTB42 cells **(Fig. 7C, Table 4)**. Tenascin-C (TNC) promotes inflammatory response by inducing the expression of multiple pro-inflammatory factors in innate immune cells such as microglia and macrophages. TNC drives macrophage differentiation and polarization predominantly towards an M1-like phenotype [22]. PZP cell lines showed low expression of TNC, epithelial cell lines displayed high expression, while synergistically increased expressions were observed under co-culture of KTB39 and PZP cells,

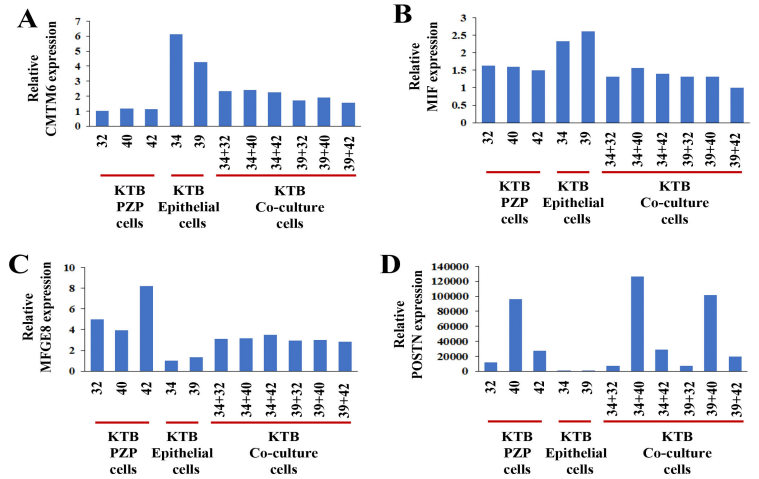

Fig. 8: Effect of co-culture of PZP and luminal progenitor cell lines on expression of genes. Expression of CMTM6 (A), MIF (B), MFGE8 (C), and POSTN (D) in PZP cell lines (KTB32, KTB40, KTB42), luminal progenitor (epithelial cells; KTB34, KTB39), and co-culture of PZP and luminal progenitor cell lines.

but no effect was found under co-culture of KTB34 and PZP cells **(Fig. 7D, Table 4)**. Note that KTB39 is a basal-like cell line derived from AA, whereas KTB34 is a luminal A type cell line from Caucasian women. Thus, co-culturing of PZP and epithelial cells revealed epithelial cell type-dependent production of TNC. CSF1 is a cytokine that has macrophage function–promoting properties. Production of CSF1 controls both the differentiation and immune regulatory function macrophages [23]. PZP cell lines displayed high expression of CSF1, epithelial cell lines showed low expression, while additive expressions were observed under co-culture condition except KTB40 cells **(Fig. 7E, Table 4)**. Increased secretion of osteopontin (SPP1 or OPN) in myofibroblasts promotes macrophage M2 polarization through binding to $\alpha_v\beta_3$ and CD44, leading to activation of the STAT3/PPARγ pathway [24]. PZP cell lines displayed high expression of SPP1, epithelial cell lines showed low expression, while additive expressions were observed under co-culture condition **(Fig. 7F, Table 4)**. IL-33 is known to be upregulated in metastases-associated fibroblasts, and the upregulation of IL-33 activates type 2 inflammation in the metastatic microenvironment and facilitates eosinophils, neutrophils, and inflammatory monocytes recruitment to lung metastases [25]. Co-culturing of PZP and epithelial cells revealed inhibitory effect on IL-33 expression **(Fig. 7G, Table 4)**. IL-4 and IL-13 are the cytokines that induces the activation of M2 macrophages, which is involved in immune response, tissue remodeling and allergic immune reactions. IL-4/IL-13 *in vitro* differentiated M2a macrophages significantly increase the migratory and invasive potential of breast cancer cells [26]. PZP cell lines showed low expression of IL-4, epithelial cell lines displayed high expression, while no effect was found under co-culture of PZP and epithelial cells **(Fig. 7H, Table 4)**. CMTM6 maintains the expression of PD-L1 in tumor cells to regulate anti-tumor immunity [27]. PZP cell lines showed low expression of CMTM6, epithelial cell lines displayed high expression, while no effect was found under co-culture of PZP and epithelial cells **(Fig. 8A, Table 4)**. Macrophage migration inhibitory factor (MIF) is an essential cytokine that is involved in the regulation of macrophage function in host defense through the suppression of anti-inflammatory effects of glucocorticoids [28]. Both PZP and epithelial cell lines displayed high expression of MIF, but we did not observe any effect under co-culture condition **(Fig. 8B, Table 4)**. Secretion of MFGE8 can reprogram macrophages from an M1 (proinflammatory) to an M2 (anti-inflammatory, pro-repair) phenotype. MFGE8 also induces the production of basic fibroblast growth factor that is responsible for fibroblast migration and proliferation [29]. PZP cell lines displayed high expression of MFGE8, epithelial cell lines showed low expression, while no effect was found under co-culture of PZP and epithelial cells **(Fig. 8C, Table 4)**. Periostin (POSTN) is predominantly secreted by stromal fibroblasts to promote the proliferation of tumor cells. POSTN is also an essential factor for macrophage recruitment in the tumor microenvironment and involved in the interactions between macrophages and cancer cells [30]. PZP cell lines displayed high expression of POSTN, epithelial cell lines showed low expression, while we observed an additive effect only under co-culture of KTB40 and epithelial cells that indicated the cell type-dependent production of POSTN **(Fig. 8D, Table 4)**. Thus, PZP cell composition in the breast could impact the levels of select chemokines/cytokines in the breast environment with consequential effects on the tumor immune environment.

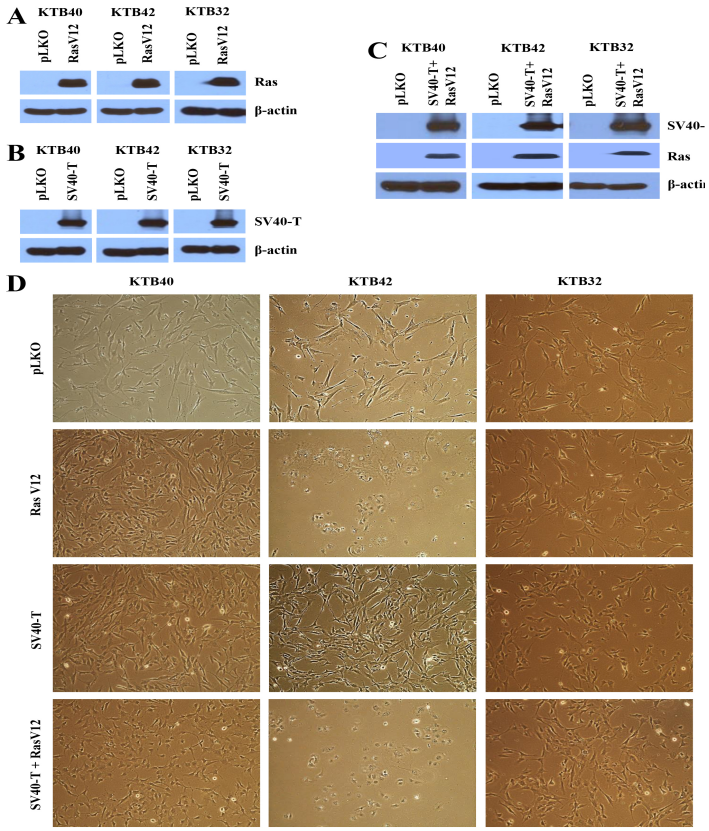

Fig. 9: (A) Western blotting was used to detect overexpression of mutant Ras in KTB32, 40 and 42. (B) Western blotting was used to detect overexpression of SV40-T antigen in KTB32, 40 and 42. (C) Western blotting was used to detect overexpression of mutant Ras and SV40-T antigen in double transformed KTB32, 40 and 42. pLKO was used as a control cell line. β–actin was used as an internal control. (D) Phase contrast images showing morphology of KTB32, KTB40 and KTB42 transformed with HRasG12V, SV40-T antigen and HRasG12V+ SV40-T.

HRas^{G12V} overexpression in PZP cells leads to trans-differentiation. Mutant Ras is one of the potent oncogenes used to transform breast epithelial cells *in vitro*. Although initially considered not a relevant oncogene in breast cancer, recent studies have clearly shown the role of Ras oncogene in endocrine resistance and metastasis of luminal breast cancer [31]. HRas^{G12V} overexpression often activates senescence program and once the senescence barrier is lost, transformation can be achieved. SV40T antigen overexpression results in inactivation of two tumor suppressor genes retinoblastoma and p53 [32]. Inactivation of retinoblastoma is observed in luminal B breast cancer, whereas p53 loss/mutation is common in triple negative breast cancers [33, 34]. PZP KTB cell lines were transformed with HRas^{G12V}, SV40-T antigen and in combination of both HRas^{G12V} and SV40-T antigen using lentivirus, since this combination is the most effective in breast epithelial cell transformation [35]. Western blotting was used to detect the overexpression of mutant HRas^{G12V} in KTB40, KTB42 and KTB32 **(Fig. 9A)**, SV40-T antigen in KTB40, KTB42 and KTB32 **(Fig. 9B)**, and combination of both HRas^{G12V} and SV40-T in KTB40, KTB42 and KTB32 **(Fig. 9C)** to ensure that transformation is oncogene driven but not spontaneous. Phase contrast images of PZP transformed cell lines (KTB40, KTB42 and KTB32) are shown in **Fig. 9D**. Transformation of PZP cells with activated HRas^{G12V} increased the fraction of cells that have acquired epithelial phenotype and express EpCAM, particularly in KTB42 **(Fig. 9D and 10).** PZP transformed cells expressed the stem/basal cell marker CD49f with inter-individual variability **(Fig. 10B).** Transformation also altered the cell surface profiles of mesenchymal stem cell marker CD90 **(Fig. 10C)**. Transformed PZP cells were CD201+ and CD44+ **(Fig. 11A and B)**. Thus, PROCR+/EpCAM-/ZEB1+ subpopulation of breast cells corresponds to a unique population of cells with the capability of trans-differentiation upon transformation.

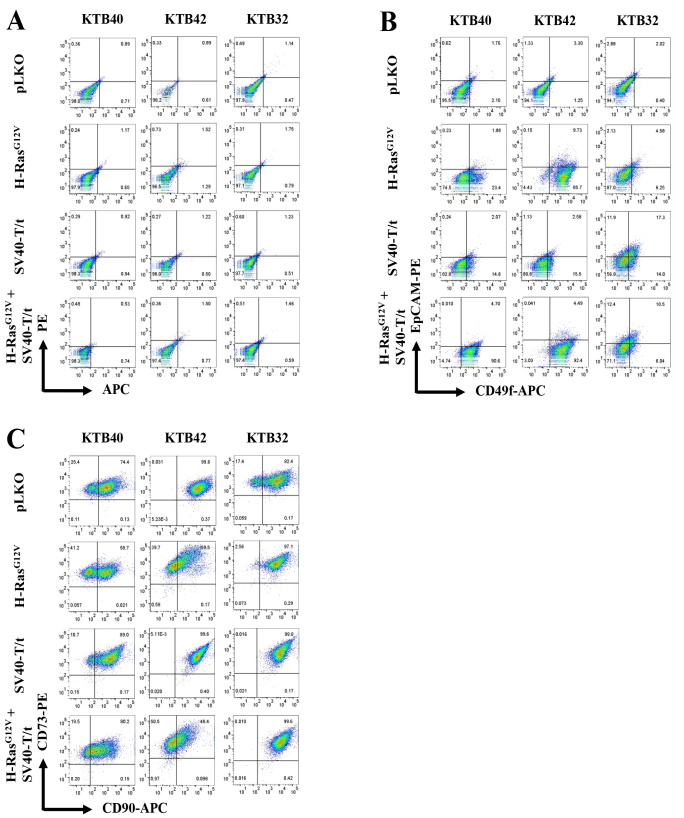

Fig. 10: (A) APC and PE isotypes controls of cell lines characterized by flow cytometry. These staining patterns were used to draw quadrants. (B) CD49f and EpCAM staining patterns of immortalized and transformed KTB32, KTB40 and KTB42 cell lines. CD49f+/EpCAM-, CD49f+/EpCAM+ and CD49f-/EpCAM+ cells correspond to stem/basal, progenitor and differentiated cells, respectively. (C) CD90 and CD73 staining patterns of immortalized and transformed KTB32, KTB40 and KTB42 cell lines.

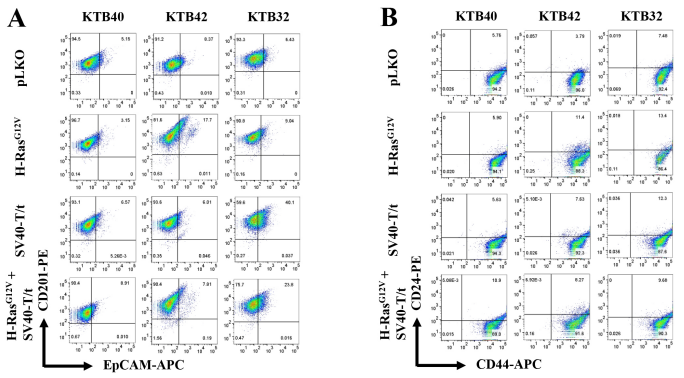

Fig. 11: (A) CD201 and EpCAM staining patterns of immortalized and transformed KTB32, KTB40 and KTB42 cell lines. (B) CD44 and CD24 staining patterns of immortalized and transformed KTB32, KTB40 and KTB42 cell lines.

PROCR+/ZEB1+/PDGFRα cells transformed with Ras and SV40T-antigen are tumorigenic in NSG mice. Since transformation of PROCR+/ZEB1+ cells resulted in epithelial trans-differentiation and cells acquired CD49f positivity, we next determined whether cells expressing oncogenes are tumorigenic in NSG mice. Indeed, five million transformed cells in 50% matrigel implanted into the mammary gland of 6-7 week old female NSG (NOD/SCID/IL2Rgnull) mice progressed into tumors. Tumor was resected and analyzed by H&E staining and expression of estrogen receptor alpha (ERα), GATA3, FOXA1, CK5/6, CK8, CK14 and CK19 using immunohistochemistry. ERα-FOXA1-GATA3 transcription factor network is generally expressed in hormonally responsive luminal cells [36]. The luminal cells express cytokeratin 19 (CK19), while basal cell types express

cytokeratin 5/6 (CK5/6) and cytokeratin 14 (CK14), and cells expressing both CK14 and CK19 show luminal progenitor phenotype [37]. KTB42-HRas^{G12V} cell-derived tumor was ERα-/GATA3-/FOXA1+ **(Fig. 12A).** Surprisingly, KTB42-HRas^{G12V}-derived tumor was CK5/6-/CK8-/CK14-/CK19- **(Fig. 12C)**. KTB42 cell line transformed with both mutant HRas^{G12V} and SV40-T antigen also developed tumors in NSG mice. KTB42-

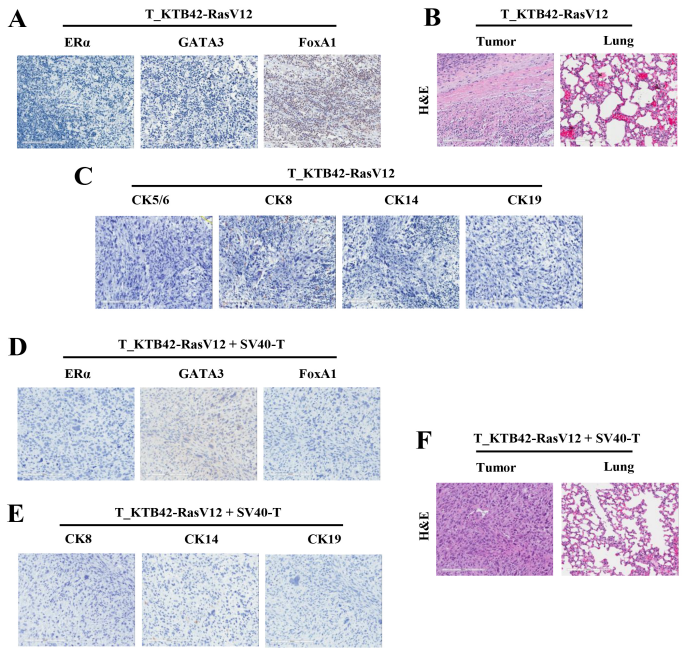

Fig. 12: (A) Immunohistochemistry (IHC) analyses of luminal markers ERα, GATA3 and FOXA1 in tumors developed from the KTB42-HRasG12V transformed cells. (B) Tumor developed from KTB42-HRasG12V transformed cells metastasized to lungs. (C) IHC analyses of cytokeratins CK5/6, CK14, CK8 and CK19 in tumors developed from the KTB42-HRasG12V transformed cells. Basal marker: CK5/6 and CK14, Luminal marker: CK8 and CK19. (D) IHC analyses of luminal markers ERα, GATA3 and FOXA1 in tumors developed from the KTB42-HRasG12V+SV40-T antigen transformed cells. (E) IHC analyses of cytokeratins CK14, CK8 and CK19 in tumors developed from the KTB42-HRasG12V+SV40-T antigen transformed cells. (F) H&E staining shows the type of tumors. Representative IHC data are shown.

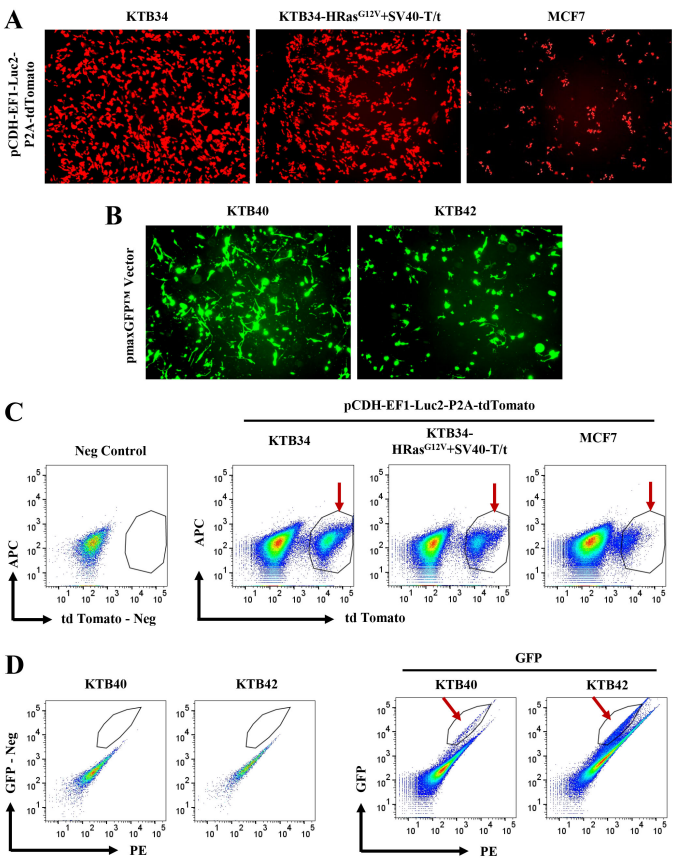

Fig. 13: (A) KTB34, KTB34-HRas^{G12V}+SV40-T/t transformed and MCF7 cells were transduced with lentivirus expressing tdTomato. (B) KTB40 and KTB42 were transfected with GFP expressing vector. (C) tdTomato expressing KTB34, KTB34-HRas^{G12V}+SV40-T/t transformed and MCF7 cells were sorted by flow cytometry. (D) GFP expressing KTB40 and KTB42 cells were sorted by flow cytometry.

HRasG12V+SV40-T cell-derived tumor was ERα-/GATA3-/FOXA1- **(Fig. 12D)**, CK5/6-/CK14-/CK19- **(Fig. 12E)**. Unlike luminal breast epithelial cell derived tumors obtained after transformation with the same set of oncogenes [38], which metastasized to lungs, these tumors did not show extensive lung metastasis **(Fig. 12B and F).** Histologically, these tumors are pleomorphic anaplastic sarcomas, which comprise 0.5-1% of all breast neoplasms **(Fig. 12F)** [39]. Thus, PROCR+/EpCAM- cells, enriched in AA women, can undergo transformation.

The effects of trans-differentiated PZP cells on invasiveness and drug sensitivity of various breast cancer cell lines: We were generated tdTomato-labeled KTB34, KTB34-HRas^{G12V}+SV40-T/t transformed and MCF7 cell line using pCDH-EF1-Luc2-P2A-tdTomato lentivirus **(Fig. 13A)**, and GFP-labeled KTB40 and KTB42 cell lines using pmaxGFP™ Vector **(Fig. 13B)**. The tdTomato and GFP-labeled cells were sorted by flow cytometry **(Fig. 13C and D)**. The goal of these experiments is to determine whether trans-differentiated PZP cells alter invasiveness as well as sensitivity of tumor cells to commonly used drugs. The tdTomato-labeled cell lines will be co-cultured with GFP-labeled undifferentiated PZP cells or trans-differentiated into fibroblasts, epithelial, adipocytes, and osteoblasts in a Boyden chamber and invasion of cancer cells will be measured. These cell lines will be used to study the effects of trans-differentiated PZP cells on growth and metastatic properties of breast cancer cells in vivo.

Specific aim 2: To investigate the role of hyperactive c-MET signaling in breast tumorigenesis under duffy-null background

Progress:

Creation of immortalized and transformed breast epithelial cells from AA women under wild type and duffy heterozygous genetic background: We screened DNA from 50 AA women, who donated breast tissues for research for duffy phenotype. Twenty donors carried duffy heterozygous and one donor carried duffy-null genome. We generated breast epithelial cells from five duffy heterozygous and five duffy wild type donors. Unfortunately, we did not obtain enough cells from many of them. However, we were successful in establishing immortalized cell line from one of the duffy heterozygous donor (KTB41) and we already have immortalized cell lines from three duffy wild type AA donors (KTB8, KTB39 and KTB51). Cells from two other duffy-heterozygous donors are currently being immortalized.

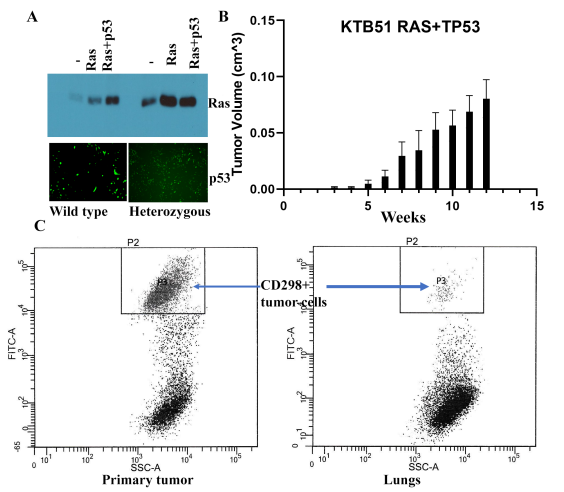

Fig. 14: Generation of transformed duffy-wild type and duffy-heterozygous cells using HRASG12V and TP53R273C. A) Expression levels of Ras(top) and p53 (bottom) in transformed cells. B) Growth rate of HRasG12V+TP53R273C expressing duffy-wild type cells in NSG mice. C) Both tumors and lungs contain CD298+ human cells indicating lung metastasis.

Breast epithelial cells transformed with HRas^{G12V} plus TP53^{R273C} are tumorigenic: We have routinely used HRas^{G12V} plus SV40-T/t antigens to obtain transformation of breast epithelial cells but use of SV40-T/t antigens is often criticized for lack of human relevance [38]. Therefore, we generated immortalized KTB51 and KTB41 cells overexpressing HRas^{G12V} or PIK3CA^{H1047R} plus TP53^{R273C}. HRas^{G12V} expression in cell lines is shown in **Fig. 14A.** Since TP53^{R273C} expression vector contained GFP, p53 expression was visualized through GFP-positivity. KTB51 cells transformed with HRas^{G12V} plus TP53^{R273C} but not PIK3CA^{H1047R} plus TP53^{R273C} formed tumors in NSG mice **(Fig. 14B).** These tumors metastasize to lungs as a fraction of cells cultured from lung tissues were positive for human specific CD298 **(Fig. 14C)**. We are in the process of establishing tumor and metastasis-derived cell lines. Similar studies with KTB41 derivatives are currently underway. Thus, we have established a system to delineate differences in tumor characteristics under duffy-wild type and duffy-heterozygous phenotype to pursue studies described in this aim.

We also performed receptor tyrosine kinase phospho-array to determine whether there are any differences in signaling between duffy wild type and duffy-heterozygous cells. We found specific increase in tyrosine phosphorylation of FGFR3 in duffy-heterozygous cells compared to duffy-wild type cells **(Fig. 15).** Ongoing studies with transformed cells will indicate whether such differences in signaling networks exist in tumors *in vivo*.

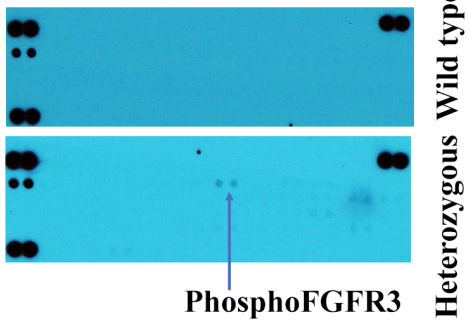

Fig. 15: RTK array shows specific phosphorylation of FGFR3 in duffy-heterozygous cells compared to duffy-wild type cells.

Impact: The influence of adipogenic progenitors and the duffy-null phenotype on the normal breast and breast cancer biology of women of African descent.

1) Results presented in Aim 1 further confirmed enrichment of PZP cells (IHCs with PROCR, ZEB1 and PDGFRα) in the breast tissues of AA women compared to Caucasian or Latina women. These cells, while themselves can be transformed to generate metaplastic tumors, have the potential to alter tumor microenvironment, which may impact immune cell composition of the breast. It is likely that the normal breast and breast tumors of AA women have higher local levels of IL-6 and TAGLN, which can have an impact on immune cell recruitment. Therefore, evaluation of breast tumors in AA women may require the assessment of IL-6. PZP cells themselves are heterogenous population of cells requiring further characterization.

2) Based on preliminary results of Aim 2, basal and transformation-induced signaling pathway activation under duffy-wild type and duffy-heterozygous genetic background is different. Thus, AA women should not be clubbed into one genetic ancestry category and evaluating AA women for duffy phenotype (40% of AA women are duffy-heterozygous or duffy-null) should help to predict metastasis and design better treatment options.

Challenges and Problems: We are encountering some difficulty in immortalizing duffy-null cells. This is mainly due to outgrowth of fibroblast-like cells leading to selective loss of epithelial cells. We plan to process additional samples with hope to resolve this issue.

Products: Due to COVID-19 travel restrictions, we did not present results in any events. However, a manuscript describing parts of the results with acknowledgment to this funding has just been published online.

Kumar B, Bhat-Nakshatri P, Maguire C, Jacobsen M, Temm CJ, Sandusky G and Nakshatri H. (2021). Bidirectional regulatory cross-talk between cell context and genomic aberrations shapes breast tumorigenesis. **Molecular Cancer Research in press.**

Participants & Other Collaborating Organizations: All participants are from IU
Brijesh Kumar
Katie Batic
Poornima Bhat-Nakshatri
Sandra Althouse
Maggie Granatir
George Sandusky
Anna Maria Storniolo
Natascia Marino

Special Reporting Requirements: None

Appendices: Manuscript in press

References:

1. Nakshatri H, *et al.* Genetic ancestry-dependent differences in breast cancer-induced field defects in the tumor-adjacent normal breast. *Clin Cancer Res* **25**, 2848-2859 (2019).

2. Nievergelt CM, *et al.* Inference of human continental origin and admixture proportions using a highly discriminative ancestry informative 41-SNP panel. *Investig Genet* **4**, 13 (2013).

3. Wang D, *et al.* Identification of multipotent mammary stem cells by protein C receptor expression. *Nature* **517**, 81-84 (2014).

4. Nakshatri H, Anjanappa M, Bhat-Nakshatri P. Ethnicity-Dependent and -Independent Heterogeneity in Healthy Normal Breast Hierarchy Impacts Tumor Characterization. *Scientific reports* **5**, 13526 (2015).

5. Joshi PA, *et al.* PDGFRalpha(+) stromal adipocyte progenitors transition into epithelial cells during lobulo-alveologenesis in the murine mammary gland. *Nature communications* **10**, 1760 (2019).

6. Cardiff RD, Wellings SR. The comparative pathology of human and mouse mammary glands. *J Mammary Gland Biol Neoplasia* **4**, 105-122 (1999).

7. Morsing M, *et al.* Evidence of two distinct functionally specialized fibroblast lineages in breast stroma. *Breast Cancer Res* **18**, 108 (2016).

8. Morsing M, *et al.* Fibroblasts direct differentiation of human breast epithelial progenitors. *Breast Cancer Res* **22**, 102 (2020).

9. Prasad M, *et al.* Dual TGFbeta/BMP Pathway Inhibition Enables Expansion and Characterization of Multiple Epithelial Cell Types of the Normal and Cancerous Breast. *Mol Cancer Res* **17**, 1556-1570 (2019).

10. Al-Hajj M, Wicha MS, Benito-Hernandez A, Morrison SJ, Clarke MF. Prospective identification of tumorigenic breast cancer cells. *Proc Natl Acad Sci U S A* **100**, 3983-3988 (2003).

11. Morel AP, *et al.* A stemness-related ZEB1-MSRB3 axis governs cellular pliancy and breast cancer genome stability. *Nat Med* **23**, 568-578 (2017).

12. Su S, *et al.* CD10(+)GPR77(+) Cancer-Associated Fibroblasts Promote Cancer Formation and Chemoresistance by Sustaining Cancer Stemness. *Cell* **172**, 841-856 e816 (2018).

13. Visvader JE, Stingl J. Mammary stem cells and the differentiation hierarchy: current status and perspectives. *Genes Dev* **28**, 1143-1158 (2014).

14. Rao D, Kimler BF, Nothnick WB, Davis MK, Fan F, Tawfik O. Transgelin: a potentially useful diagnostic marker differentially expressed in triple-negative and non-triple-negative breast cancers. *Hum Pathol* **46**, 876-883 (2015).

15. Tawfik O, Rao D, Nothnick WB, Graham A, Mau B, Fan F. Transgelin, a Novel Marker of Smooth Muscle Differentiation, Effectively Distinguishes Endometrial Stromal Tumors from Uterine Smooth Muscle Tumors. *Int J Gynecol Obstet Reprod Med Res* **1**, 26-31 (2014).

16. Holloway EM, *et al.* Mapping Development of the Human Intestinal Niche at Single-Cell Resolution. *Cell Stem Cell* **28**, 568-580 e564 (2021).

17. O'Grady S, Morgan MP. Microcalcifications in breast cancer: From pathophysiology to diagnosis and prognosis. *Biochim Biophys Acta Rev Cancer* **1869**, 310-320 (2018).

18. Chen X, Song E. Turning foes to friends: targeting cancer-associated fibroblasts. *Nat Rev Drug Discov* **18**, 99-115 (2019).

19. Bhat-Nakshatri P, Newton TR, Goulet R, Jr., Nakshatri H. NF-kappaB activation and interleukin 6 production in fibroblasts by estrogen receptor-negative breast cancer cell-derived interleukin 1alpha. *Proc Natl Acad Sci U S A* **95**, 6971-6976 (1998).

20. Liao X, *et al.* WISP1 Predicts Clinical Prognosis and Is Associated With Tumor Purity, Immunocyte Infiltration, and Macrophage M2 Polarization in Pan-Cancer. *Front Genet* **11**, 502 (2020).

21. Tao W, *et al.* Dual Role of WISP1 in maintaining glioma stem cells and tumor-supportive macrophages in glioblastoma. *Nature communications* **11**, 3015 (2020).

22. Yalcin F, Dzaye O, Xia S. Tenascin-C Function in Glioma: Immunomodulation and Beyond. *Advances in experimental medicine and biology* **1272**, 149-172 (2020).

23. Braza MS*, et al.* Neutrophil derived CSF1 induces macrophage polarization and promotes transplantation tolerance. *Am J Transplant* **18**, 1247-1255 (2018).

24. Yuan Q*, et al.* MyD88 in myofibroblasts enhances colitis-associated tumorigenesis via promoting macrophage M2 polarization. *Cell reports* **34**, 108724 (2021).

25. Shani O*, et al.* Fibroblast-Derived IL33 Facilitates Breast Cancer Metastasis by Modifying the Immune Microenvironment and Driving Type 2 Immunity. *Cancer Res* **80**, 5317-5329 (2020).

26. Little AC*, et al.* IL-4/IL-13 Stimulated Macrophages Enhance Breast Cancer Invasion Via Rho-GTPase Regulation of Synergistic VEGF/CCL-18 Signaling. *Frontiers in oncology* **9**, 456 (2019).

27. Burr ML*, et al.* CMTM6 maintains the expression of PD-L1 and regulates anti-tumour immunity. *Nature* **549**, 101-105 (2017).

28. Calandra T, Bucala R. Macrophage Migration Inhibitory Factor (MIF): A Glucocorticoid Counter-Regulator within the Immune System. *Crit Rev Immunol* **37**, 359-370 (2017).

29. Laplante P*, et al.* MFG-E8 Reprogramming of Macrophages Promotes Wound Healing by Increased bFGF Production and Fibroblast Functions. *J Invest Dermatol* **137**, 2005-2013 (2017).

30. Ma H*, et al.* Periostin Promotes Colorectal Tumorigenesis through Integrin-FAK-Src Pathway-Mediated YAP/TAZ Activation. *Cell reports* **30**, 793-806 e796 (2020).

31. Wright KL*, et al.* Ras Signaling Is a Key Determinant for Metastatic Dissemination and Poor Survival of Luminal Breast Cancer Patients. *Cancer Res* **75**, 4960-4972 (2015).

32. Elenbaas B*, et al.* Human breast cancer cells generated by oncogenic transformation of primary mammary epithelial cells. *Genes Dev* **15**, 50-65. (2001).

33. Witkiewicz AK, Knudsen ES. Retinoblastoma tumor suppressor pathway in breast cancer: prognosis, precision medicine, and therapeutic interventions. *Breast Cancer Res* **16**, 207 (2014).

34. Cancer Genome Atlas N. Comprehensive molecular portraits of human breast tumours. *Nature* **490**, 61-70 (2012).

35. Ince TA*, et al.* Transformation of different human breast epithelial cell types leads to distinct tumor phenotypes. *Cancer Cell* **12**, 160-170 (2007).

36. Eeckhoute J, Keeton EK, Lupien M, Krum SA, Carroll JS, Brown M. Positive cross-regulatory loop ties GATA-3 to estrogen receptor alpha expression in breast cancer. *Cancer Res* **67**, 6477-6483 (2007).

37. Villadsen R*, et al.* Evidence for a stem cell hierarchy in the adult human breast. *J Cell Biol* **177**, 87-101 (2007).

38. Kumar B*, et al.* Bidirectional regulatory crosstalk between cell context and genomic aberrations shapes breast tumorigenesis. *Mol Cancer Res*, (2021).

39. Pandey M, Mathew A, Abraham EK, Rajan B. Primary sarcoma of the breast. *J Surg Oncol* **87**, 121-125 (2004).

Bidirectional Regulatory Cross-talk Between Cell Context and Genomic Aberrations Shapes Breast Tumorigenesis

Brijesh Kumar[1], Poornima Bhat-Nakshatri[1], Calli Maguire[2], Max Jacobsen[2], Constance J. Temm[2], George Sandusky[2], and Harikrishna Nakshatri[1,3,4]

ABSTRACT

Breast cancers are classified into five intrinsic subtypes and 10 integrative clusters based on gene expression patterns and genomic aberrations, respectively. Although the cell-of-origin, adaptive plasticity, and genomic aberrations shape dynamic transcriptomic landscape during cancer progression, how interplay between these three core elements governs obligatory steps for a productive cancer progression is unknown. Here, we used genetic ancestry-mapped immortalized breast epithelial cell lines generated from breast biopsies of healthy women that share gene expression profiles of luminal A, normal-like, and basal-like intrinsic subtypes of breast cancers and breast cancer relevant oncogenes to develop breast cancer progression model. Using flow cytometry, mammosphere growth, signaling pathway, DNA damage response, and *in vivo* tumorigenicity assays, we provide evidence that establishes cell context–dependent effects of oncogenes in conferring plasticity, self-renewal/differentiation, intratumor heterogeneity, and metastatic properties. In contrast, oncogenic aberrations, independent of cell context, shaped response to DNA damage-inducing agents. Collectively, this study reveals how the same set of genomic aberration can have distinct effects on tumor characteristics based on cell-of-origin of tumor and highlights the need to utilize multiple "normal" epithelial cell types to decipher oncogenic properties of a gene of interest. In addition, by creating multiple isogenic cell lines ranging from primary cells to metastatic variants, we provide resources to elucidate cell-intrinsic properties and cell-oncogene interactions at various stages of cancer progression.

Implications: Our findings demonstrate that how an interplay between the normal cell type that encountered genomic aberrations and type of genomic aberration influences heterogeneity, self-renewal/differentiation, and tumor properties including propensity for metastasis.

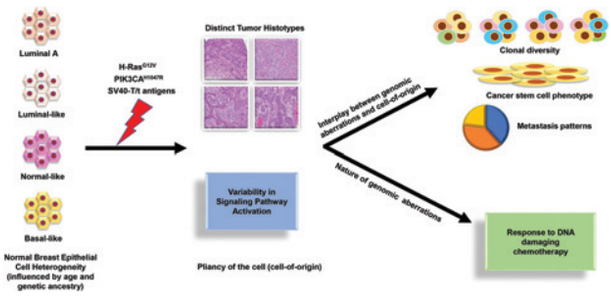

Introduction

Molecular profiling of breast tumors has revealed different intrinsic subtypes (1), which include estrogen receptor alpha (ERα)-positive luminal A and luminal B subtypes, HER2$^+$, basal-like and normal-like subtypes. These subtypes of breast cancers have heterogeneous pathologies and different clinical outcome. Similarly, based on genomic aberrations, breast cancers are classified into 10 integrative clusters with distinct outcomes (2). Molecular basis for differing outcomes from different subtypes/clusters is unclear but could be related to interplay between cell-of-origin of tumors and genomic aberrations (3). The normal breast contains different subpopulations of cells, such as stem cells, luminal-progenitor cells, and luminal-differentiated cells. It is proposed that luminal progenitors or bipotent progenitors are the cell-of-origin of basal breast cancers (4–6). HER2$^+$ cancers may originate from late luminal progenitors, whereas luminal A and luminal B breast cancers may arise from luminal-differentiated cells (3). Through integration of single-cell sequencing data of healthy breast with publicly available breast cancer gene expression datasets, we recently proposed that the majority of breast cancers originate from mature luminal cells (7). However, experimental validation of these possibilities is still challenging because most of the prior culturing methods favored the outgrowth of basal-like breast epithelial cells (8–10). Therefore, developing a model system that utilizes breast epithelial cell lines with luminal characteristics derived from multiple healthy donors would aid in establishing relationship between cell-of-origin, genomic aberrations, and obligatory steps in breast cancer progression.

The normal breast cells progress to cancer due to acquisition of genetic or epigenetic alterations (5). Several breast cancer subtype specific mutations have been reported including *PIK3CA* mutations in luminal A/B breast cancers, loss of retinoblastoma gene in luminal B breast cancers, and *PIK3CA* amplifications and *TP53* mutations in basal-like breast cancers (11). *HER2* amplification is observed in 15% of breast cancers. To date, none of these oncogenic mutations could reproducibly transform breast epithelial cells *in vitro* and therefore,

[1]Departments of Surgery, Indiana University School of Medicine, Indianapolis, Indiana. [2]Department of Pathology and Laboratory Medicine, Indiana University School of Medicine, Indianapolis, Indiana. [3]Department of Biochemistry and Molecular Biology, Indiana University School of Medicine, Indianapolis, Indiana. [4]VA Roudebush Medical Center, Indianapolis, Indiana.

Note: Supplementary data for this article are available at Molecular Cancer Research Online (http://mcr.aacrjournals.org/).

Corresponding Author: Harikrishna Nakshatri, Department of Surgery, Indiana University School of Medicine, C218C, 980 West Walnut St, Indianapolis, IN 46202. Phone: 317-278-2238; Fax: 317-274-0396; E-mail: hnakshat@iupui.edu

Mol Cancer Res 2021;XX:XX–XX

doi: 10.1158/1541-7786.MCR-21-0163

mutated *RAS* oncogene in combination with SV40 T/t antigens still remain oncogenes of choice for transformation of breast epithelial cells (12, 13). Although initially considered not a relevant oncogene in breast cancer, recent studies have clearly shown the role of *RAS* oncogene in resistance to endocrine and CDK inhibitor therapies and metastasis of luminal breast cancer (14, 15). Simian virus 40-T/t (SV40-T/t) antigens overexpression results in inactivation of tumor suppressor genes retinoblastoma and *p53* by the large-T antigen and protein phosphatase 2A (PP2A) by the small-t- antigen (13, 16). All three of these signaling pathways are frequently aberrant in breast cancers, as evident from high frequency *p53* mutations and *PP2A* inactivation in integrative cluster 9 subtype of breast cancer (2, 10, 17), thus justifying the use of the SV40-T/t antigens in mechanistic studies relevant to breast cancer.

We took advantage of our recently developed model system of immortalized breast epithelial cell lines derived from healthy breast tissue of women to address interplay between cell-context and oncogenic aberrations on individual steps of breast cancer progression. Model and results presented in this study differ significantly from previous studies related to cell-of-origin of breast cancer (9, 12), as cells were derived from multiple healthy donors of different genetic ancestry. At the time of transformation, these cell lines were diploid in nature (18). Although these cell lines contained heterogenous population cells, RNA sequencing followed by PAM50 classification categorized the cell lines into "normal" counterparts of intrinsic subtypes. This diversity in cell characteristics allowed us to discern a strategy to systematically determine how cell-of-origin impacts phenotype of cancer cells with similar genomic aberrations. We demonstrate that interplay between cell-of-origin and genomic aberrations determine stem/progenitor/mature cell hierarchy, self-renewal/differentiation, and metastasis patterns of resulting tumors. Surprisingly, oncogenic aberrations, irrespective of the cell-of-origin of transformed cells, have a direct influence on response to chemotherapeutic drugs. Overall, these findings advance our understanding of interplay between susceptible epithelial cell population and genomic aberrations.

Materials and Methods

Cell culture, cell line generation, and lentiviral transduction

Immortalized breast epithelial cell lines were cultured as described previously (18). Cells were transformed with oncogenes *H-Ras*^{G12V}, *PIK3CA*^{H1047R}, and SV40-T/t antigens expressing lentiviruses using vectors pLenti CMV-RasV12-Neo (w108-1; HRAS G12V, #22259, Addgene), pLenti MNDU3-PGK–PIK3CA^{H1047R}-YFP (10), and pLenti-CMV/TO-SV40 small + Large T (w612-1; #22298, Addgene), respectively. Cell lines in the laboratory are usually tested for *Mycoplasma* once in 6 months (Lonza mycoplasma testing kit, last testing was done on January 20, 2021) and cell line authentication/cross-contamination yearly using marker short tandem repeat DNA sequencing method (IDEXX BioAnalytics, last testing was done on July 30, 2020). Additional details of cell culture are provided in Supplementary Materials and Methods.

Antibodies and Western blotting

Cell lysates were prepared in radioimmunoassay buffer and analyzed by Western blotting as described previously (19). Additional details are provided in Supplementary Materials and Methods.

Flow cytometry analysis and cell sorting

Flow cytometry was performed as described previously (18). Samples were analyzed and sorted using BD FACSAria and SORPAria. Additional details are provided in Supplementary Materials and Methods.

Cell proliferation assay and mammosphere formation assay

For cell proliferation assay, cells were seeded in 96-well plates and grown for 3 days. The mammosphere formation assay was carried out to evaluate the stemness/self-renewal/differentiation properties of cells as described previously (18). Phase contrast images were captured, counted, and processed for staining at day 5. Additional details are provided in Supplementary Materials and Methods.

Xenograft study

The Indiana University Animal Care and Use Committee approved the use of animals in this study and all procedures were performed as per NIH guidelines. Transformed cells with 50% basement membrane matrix type 3 (3632-005-02, Trevigen) were implanted into the mammary fat pad of 5 to 6 weeks old female NSG (NOD/SCID/IL2Rgnull) mice. Tumor growth was measured weekly and tumor volume was calculated as described previously (20). Additional details are provided in Supplementary Materials and Methods.

IHC

Hematoxylin and eosin (H&E), ERα, GATA3, FOXA1, CK5/6, CK8, CK14, CK19, and EGFR immunostaining was performed at the Clinical Laboratory Improvement Amendments–certified Indiana University Health Pathology Laboratory and the whole-slide digital imaging system of Aperio (ScanScope CS) was used for imaging according to protocol described previously (21). Additional details are provided in Supplementary Materials and Methods.

Soft agar colony formation assay and Annexin V/dead cell apoptosis assay

A total of 20,000 cells were resuspended in 0.3% low melting point agarose (214220, BD Biosciences) containing DMEM/F-12 and 10% FBS and plated on top of 0.6% agarose bottom layer containing DMEM/F-12 and 10% FBS in 6-well plates. For Annexin V/Dead cell apoptosis assay, after the indicated drug treatment, cells were collected by trypsinization and stained with Annexin V-FITC and propidium iodide (PI) using FITC Annexin V/dead cell apoptosis kit (V13242; Invitrogen molecular probes) according to the manufacturer's instructions. Additional details are provided in Supplementary Materials and Methods.

Electrophoretic mobility shift assay

Electrophoretic mobility shift assay with whole-cell extracts from immortalized and transformed cell lines was performed as described previously (19). Additional details are provided in Supplementary Materials and Methods.

Immunofluorescence

Immunofluorescence was carried out as described previously (18). Images were acquired using an Olympus FV10000 MPE inverted confocal microscope and analyzed using Olympus software. Additional details are provided in Supplementary Materials and Methods.

Drug-sensitivity colony assay

A total of 1,000 cells were seeded in 6-well plate, treated with indicated drug for 48 hours, replaced with regular media and allowed to grow for 7 days. Colonies were stained with Coomassie brilliant blue, imaged under microscope and counted by ImageJ software.

Statistical analysis

Statistical analyses were conducted using Prism software program (version 6.0). Data were analyzed using one-way ANOVA. *P* values below 0.05 were considered statistically significant.

Results

Transformation of immortalized normal breast epithelial cell lines corresponding to intrinsic subtypes

Luminal A (KTB34), luminal-like (KTB6), normal-like (KTB39), and basal-like (KTB22) intrinsic subtypes of immortalized normal breast epithelial cell lines derived from breast biopsies of healthy women described in our previous study (18) were transformed with *H-Ras*^{G12V}, SV40-T/t antigens or combination of both oncogenes using lentivirus-mediated gene transfer. **Fig. 1A** provides schematic view of the experimental design. *H-Ras*^{G12V} overexpression initiated senescence program at first in all cell lines but eventually transformed clones emerged. Expression levels of oncogenes were similar across cell lines (**Fig. 1B–D**) and phase contrast images of the transformed cell lines did not reveal cell line–specific variations in phenotype as all cell lines maintained epithelial morphology (Supplementary Fig. S1A). To determine the effect of *H-Ras*^{G12V}, SV40-T/t antigens and combinations of both on cell proliferation, BrDU-incorporation-ELISA was performed. SV40-T/t antigens promoted cell proliferation at variable levels in all cell subtypes, while *H-Ras*^{G12V} had modest effect on proliferation of luminal A and luminal-like cell lines (**Fig. 1E**).

Cell type–specific effects of signaling pathways downstream of SV40-T/t antigens on stem/progenitor/mature luminal cell hierarchy

CD49f^{+}/EpCAM^{-}, CD49f^{+}/EpCAM^{+}, and CD49f^{-}/EpCAM^{+} cells are considered as basal/stem, luminal progenitor, and mature luminal cells of the breast (22). PROCR (CD201)$^{+}$ cells have been described as multipotent stem cells of the mouse mammary gland, whereas CD271^{+} and CD44^{+}/CD24^{-} cells have been described as minor population of highly invasive cells in luminal cancers and breast cancer stem cells, respectively (23–25). To determine whether *H-Ras*^{G12V} or SV40-T/t antigens alter the phenotype of transformed cells, oncogene-overexpressing cells were analyzed by flow cytometry using the above described markers. SV40-T/t antigens overexpression had cell line–specific effects on subpopulation of cells. For example, SV40-T/t antigens altered CD49f/EpCAM staining pattern by increasing intensity of EpCAM staining, which created a subpopulation of cells that are CD49f^{+}/moderate/EpCAM^{high} and CD49f^{+}/EpCAM^{low} (**Fig. 1F**). These changes were clearly evident in luminal A and basal-like cell lines. Similar cell line–specific changes in stem/progenitor/mature cell hierarchy upon SV40-T/t antigens overexpression were observed when cells were analyzed for CD271/EpCAM, CD201/EpCAM, and CD44/CD24 expression patterns (**Fig. 1G**; Supplementary Fig. S1B–S1D). SV40-T/t antigens created a distinct CD201^{+}/EpCAM^{low} subpopulation of transformed luminal A and basal-like cell lines. Thus, SV40-T/t antigens influence stem/progenitor/differentiation hierarchy of transformed cells in a cell context–dependent manner. Unlike SV40-T/t antigens, *H-Ras*^{G12V} overexpression had modest effects on phenotype of cell lines (**Fig. 1F** and **G**; Supplementary Fig. S1C and S1D). Notably, basal-like subtype showed a modest increase in levels of CD49f^{+}/EpCAM^{-}, CD44^{+}/CD24^{-}, CD201^{+}/EpCAM^{-}, and CD271^{+}/EpCAM^{-} subpopulations (**Fig. 1F** and **G**; Supplementary Fig. S1C and S1D). The phenotype of double-transformed cells closely resembled that of cells transformed by SV40-T/t antigens with an increase in EpCAM staining intensity and cell type–specific effects on CD271^{+} subpopulation of cells (**Fig. 1F** and **G**; Supplementary Fig. S1C and S1D). Taken together, these results indicate that both cell-of-origin and oncogenic mutations determine the stem/progenitor/mature luminal cell hierarchy of transformed cells.

Interplay between cell-of-origin and oncogenes influences self-renewal/differentiation of transformed cells

Mammosphere assay is routinely used as a surrogate assay to measure self-renewal and differentiation capacity of normal and transformed cells. To determine whether transformed luminal A, luminal-like, normal-like, or basal-like subtypes show variability in stemness and differentiation properties, we performed serial dilution mammosphere assay. All transformed cells formed variable size mammospheres. SV40-T/t antigens transformed cells formed larger spheres compared to *H-Ras*^{G12V} and immortalized pLKO control cells, which is consistent with the effects of SV40-T/t on cell proliferation (**Fig. 2A** and **B**). SV40-T/t antigens transformed basal-like subtype displayed higher mammosphere-forming ability than other cell types (**Fig. 2A** and **B**). In serial dilution mammosphere assay, only SV40-T/t antigens ± *H-Ras*^{G12V} transformed cells generated tertiary mammospheres. These results suggest that SV40-T/t antigens confer enhanced self-renewal capacity to transformed cells.

Characterization of cells in primary mammospheres by flow cytometry revealed that oncogenes had cell-of-origin specific effects on subpopulation of differentiated (CD49f^{-}/EpCAM^{+} and CD44^{-}/CD24^{+}) and stem/basal (CD49f^{+}/EpCAM^{-} and CD44^{+}/CD24^{-}) cells. While immortalized and transformed counterparts of luminal A cell line displayed predominantly luminal progenitor phenotype under mammosphere growth condition, SV40-T/t antigens reduced the number of differentiated cells with the other luminal cell line as well as normal-like cell line (**Fig. 2C** and **D**). The basal-like cell line underwent dramatic changes in phenotype upon transformation with both oncogenes increasing the proportion of cells with cancer stem cell phenotype (**Fig. 2C** and **D**). Thus, cell-of-origin has a major influence on whether transformed cells maintain or acquire cancer stem cell phenotype upon transformation. Note that staining patterns of isotype controls for flow cytometry of mammosphere-derived cells are shown in Supplementary Fig. S1E, which were used for gating and to determine quadrants.

Cell context influences oncogene-induced signaling pathway activation

To extend our observations on cell of origin–dependent variability in basal and transformation-mediated signaling changes, we measured phospho-AKT (Ser473), phospho-STAT3 (Tyr705), phospho-ERK (Thr202/Tyr204), PTEN, and BRD4 protein levels and DNA-binding activity of transcription factors NFκB, OCT-1, and AP-1 in immortalized and transformed cell lines. SV40-T/t antigen reduced phospho-AKT levels in luminal A and luminal-like cell lines but not in normal-like and basal-like cell lines (**Fig. 2E**; Supplementary Fig. S2A). SV40-T/t antigens increased phospho-STAT3 in all cell lines, although there was immortalized cell line–specific variability in basal phospho-STAT3 levels (**Fig. 2E**; Supplementary Fig. S2A). Despite previous studies demonstrating inactivation or loss of PTEN in breast cancers (26), in our model system, transformation with either *H-Ras*^{G12V} or SV40-T/t antigens did not alter PTEN levels (**Fig. 2E**; Supplementary Fig. S2A). Thus, transformation in the model system used in this study is less likely reliant on PI3K-PTEN-AKT signaling axis. However, we cannot rule out possible differences in post-translational modification of PTEN between immortalized and transformed cells.

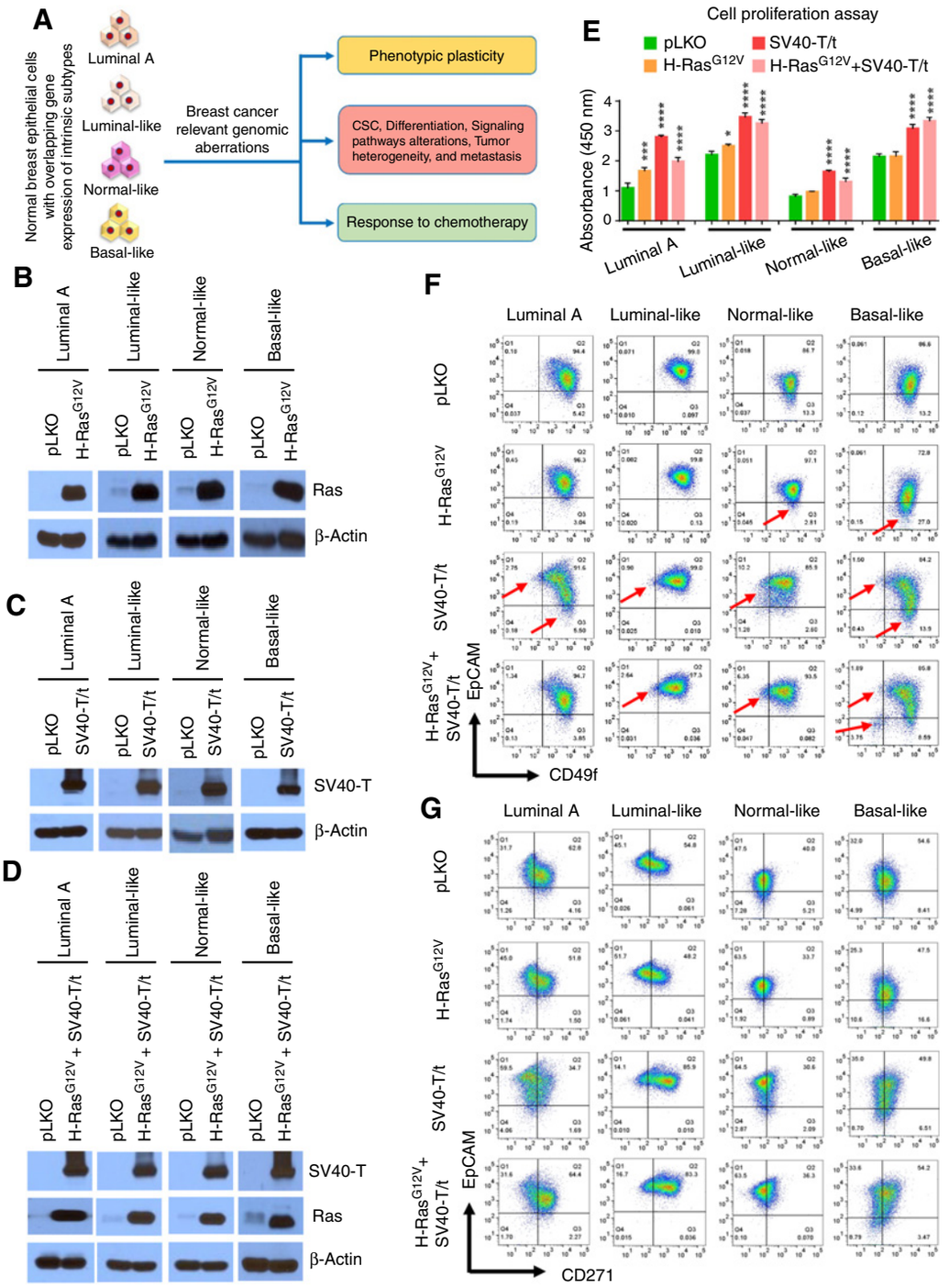

Figure 1.

Experimental design and phenotypic characterization of transformed cells. **A,** Schematic view of the experimental design. The design involved transformation of immortalized normal breast epithelial cell lines with gene expression patterns overlapping luminal A (KTB34), luminal-like (KTB6), normal-like (KTB39), and basal-like (KTB22) intrinsic subtypes with breast cancer relevant genomic aberrations. Transformed cells were examined for phenotypic plasticity, cancer stem cell (CSC) phenotype, differentiation, signaling pathways alterations, tumor heterogeneity, metastasis, and response to chemotherapy. **B,** Levels of mutant *H-Ras*^{G12V} in transduced cell lines. **C,** Levels of SV40-T antigen in the above cell lines. **D,** Levels of both *H-Ras*^{G12V} and SV40-T antigen in double-transduced cells. We first generated H-Ras^{G12V} cell lines and then introduced SV40-T antigen in most cases. **E,** SV40-T/t antigens but not *H-Ras*^{G12V} increase cell proliferation rates in all cell lines. Cell proliferation rates were determined using BrDU-incorporation-ELISA cell proliferation assay. **F,** CD49f and EpCAM staining patterns of immortalized and transformed cell lines. CD49f^{+}/EpCAM^{-}, CD49f^{+}/EpCAM^{+} and CD49f^{-}/EpCAM^{+} cells correspond to stem/basal, progenitor and differentiated cells, respectively. Q5 Red arrows indicate transformation-induced changes in phenotype of cells. **G,** CD271 and EpCAM staining patterns of immortalized and transformed cell lines.

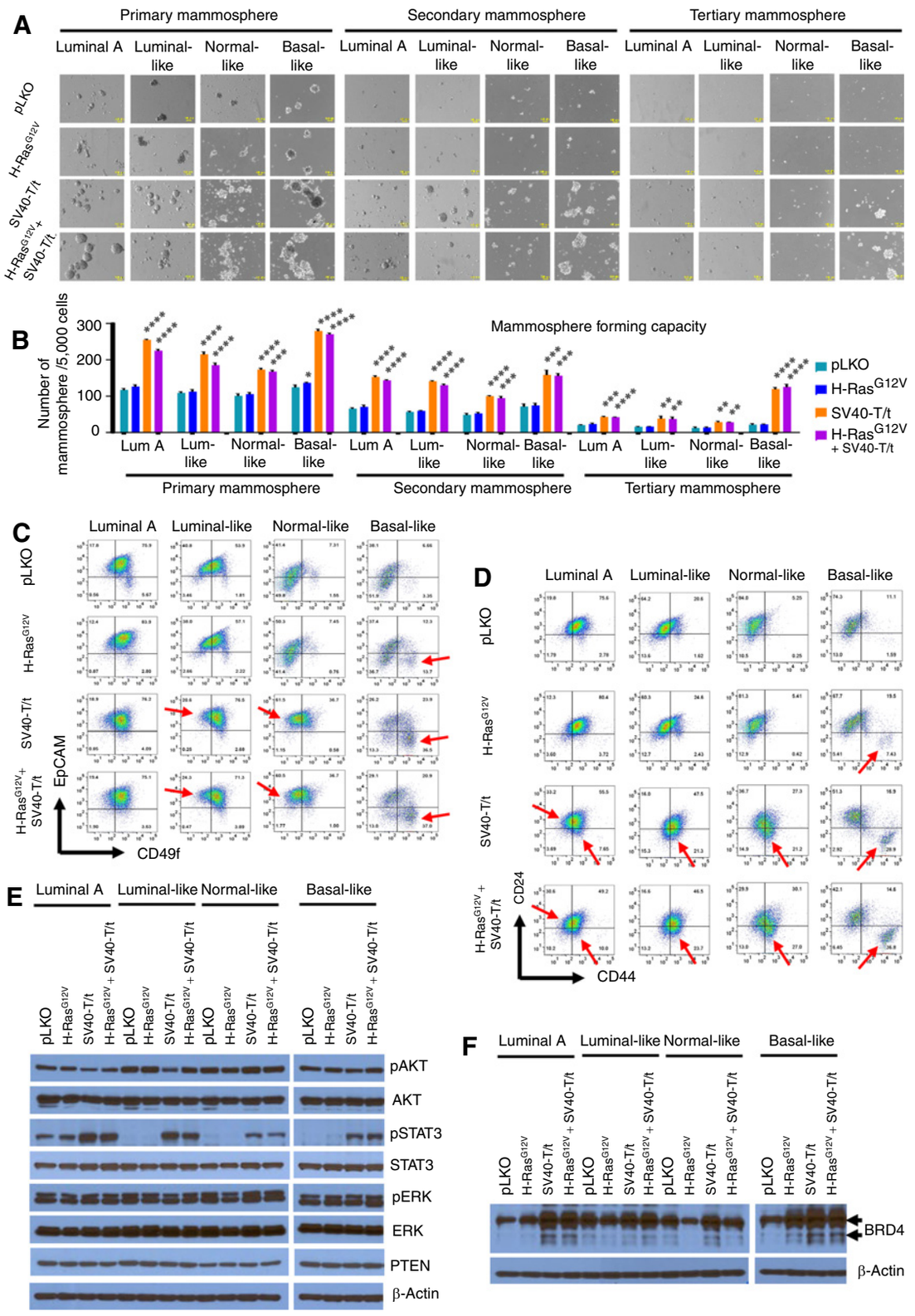
A
Primary mammosphere
Secondary mammosphere
Tertiary mammosphere
Luminal A
Luminal-like
Normal-like
Basal-like
pLKO
H-Ras G12V
SV40-T/t
H-Ras G12V + SV40-T/t
B
Mammosphere forming capacity
Number of mammosphere /5,000 cells
300
200
100
0
Lum A
Lum-like
Normal-like
Basal-like
Primary mammosphere
Secondary mammosphere
Tertiary mammosphere
pLKO
H-Ras G12V
SV40-T/t
H-Ras G12V + SV40-T/t
C
Luminal A
Luminal-like
Normal-like
Basal-like
EpCAM
CD49f
D
CD24
CD44
E
pAKT
AKT
pSTAT3
STAT3
pERK
ERK
PTEN
β-Actin
F
BRD4
β-Actin

Overexpression of *H-Ras*^{G12V} had minimum effect in NFκB DNA binding activity. However, SV40-T/t antigens increased NFκB with cell type–specific variability in the level of induction (Supplementary Fig. S2B). We did not observe an effect of oncogenes on OCT-1 and AP-1 binding activity (Supplementary Fig. S2C and S2D), which served as controls. These results suggest that while oncogenes primarily determine signaling pathway activation in transformed cells, cell-of-origin has an impact on degree of signaling pathway activation.

BET bromodomain (BRD) proteins have recently been identified as major regulators of oncogenic transcription factors and BRD4 among them has been targeted therapeutically (27). Two isoforms of BRD4 with opposing functions in cancer progression have been described: a long isoform with tumor suppressor activity and a short isoform with pro-metastatic functions (28). While SV40-T/t antigens transformed cells showed increased levels of both long and short forms of BRD4 at variable levels compared with their immortalized counterparts, *H-Ras*^{G12V} increased BRD4 only in basal-like cell line (**Fig. 2F**; Supplementary Fig. S2E). Because transformed cells expressed higher levels of BRD4 compared with immortalized cells, we examined whether immortalized and *H-Ras*^{G12V} + SV40-T/t antigens transformed luminal A and basal-like cell lines show differences in sensitivity to BRD inhibitor JQ1 (29). Transformed cells showed lower sensitivity to JQ1 compared with their immortalized cell counterparts, suggesting that BRD4 levels determine sensitivity to JQ1 (Supplementary Fig. S2F).

Tumors originating from luminal A and luminal-like but not normal-like or basal-like cell lines express luminal markers GATA3 and FOXA1

To determine whether luminal A, luminal-like, normal-like, and basal-like subtypes expressing *H-Ras*^{G12V} and SV40-T/t antigens form tumors, we injected 5×10^6 transformed cells with 50% matrigel in 100 μL Hank's Balanced Salt Solution into the mammary fat pad of 6–7 weeks old female NSG (NOD/SCID/IL2Rgnull) mice. Tumors were analyzed by H&E staining and expression of ERα, GATA3, FOXA1, CK5/6, CK8, CK14, CK19, and EGFR using IHC. We also created cell lines from half of tumors to characterize the phenotypic cellular heterogeneity using various cell surface markers. Human specific antibody against Na^+/K^+ ATPase CD298 (ATP1B3) cell surface marker was used to sort the CD298-enriched human tumor cell populations from mouse stromal cells (30).

Double-transformed luminal A (13/13), luminal-like (9/13), normal-like (10/18), and basal-like (13/14) cell lines developed tumors in mice at variable frequency and growth rates (**Fig. 3A**). Tumor incidence rate was statistically significantly higher with transformed luminal A ($P = 0.009$) and basal-like cell line ($P = 0.04$) compared with transformed normal-like cell line. Tumors displayed variable growth rates as well with transformed luminal A cell line–derived tumors displaying highest growth rate (**Fig. 3B**), demonstrating the influence of cell-of-origin on tumor progression rate. Among *H-Ras*^{G12V} alone transformed cell lines, only basal-like subtype developed tumors, that too at very low frequency, suggesting the influence of cell type on *H-Ras*^{G12V} induced transformation (Supplementary Fig. S3A). Interestingly, despite demonstrating maximum effects on stem/luminal progenitor/mature luminal cell hierarchy, proliferation rate, self-renewal capacity in mammosphere assay, and signaling pathways *in vitro*, cells overexpressing SV40-T/t antigens failed to generate tumors (Supplementary Fig. S3B). These results highlight how aggressive characteristics displayed by transformed cells *in vitro* do not translate into similar phenotypes *in vivo*.

Representative H&E staining patterns of tumors are shown in **Fig. 3C**. Consistent with phenotypic heterogeneity within cell lines observed *in vitro*, transformed luminal A cell line generated poorly differentiated carcinoma, moderately differentiated squamous cell carcinoma, well-differentiated squamous cell carcinoma and adenocarcinoma. Luminal-like double-transformed cell-derived tumors showed undifferentiated carcinoma, poorly differentiated squamous carcinoma, moderately differentiated squamous cell carcinoma, pleomorphic carcinoma with areas of multi-nucleated cells, and adenocarcinoma. Normal-like double-transformed cell-derived tumors were anaplastic carcinoma with squamous cell features, undifferentiated carcinoma, poorly differentiated squamous cell carcinoma, and anaplastic squamous sarcoma. Basal-like double-transformed cell-derived tumors showed undifferentiated squamous cell carcinoma, squamous cell carcinoma, anaplastic, adenosquamous, and adenoid cystic carcinomas. Tumor derived from *H-Ras*^{G12V} transformed basal-like cells showed undifferentiated carcinoma (Supplementary Fig. S3C).

Transformed luminal A cell-derived tumors showed ERα$^-$/GATA3$^-$/FOXA1$^+$, ERα$^-$/GATA3$^+$/FOXA1$^-$, and ERα$^-$/GATA3$^+$/FOXA1$^+$ patterns (**Fig. 3C**). Luminal-like cell-derived tumors were ERα$^-$/GATA3$^+$/FOXA1$^-$ and ERα$^-$/GATA3$^-$/FOXA1$^-$ (**Fig. 3C**). In general, adenocarcinomas were GATA3$^+$. None of the normal-like cell-derived tumors expressed luminal markers, whereas tumors derived from basal-like cell line expressed very low levels of GATA3 and FOXA1 (**Fig. 3C**). Tumor derived from *H-Ras*^{G12V} transformed basal-like cells did not express any luminal markers (Supplementary Fig. S3C). Thus, cell-of-origin rather than oncogenic aberrations determine the expression patterns of luminal cell markers in tumors.

CK5/6 but not CK14 expression patterns enabled us to distinguish luminal-like cell-derived tumors from normal-like and basal-like cell-derived tumors. The number of CK5/6$^+$ tumor cells was much higher with normal-like and basal-like cell-derived tumors compared with luminal A and luminal-like cell-derived tumors (**Fig. 3D**). Because few of the luminal A and luminal-like tumors were squamous histotypes, CK14 expression was much more common, although intensity was stronger with basal-like cell-derived tumors (**Fig. 3D**). CK19 expression was uniformly low across tumors and EGFR expression was variable and did not show any recognizable patterns. However, EGFR

Figure 2.
Interplay between cell-of-origin and oncogenes influences self-renewal/differentiation phenotype and signaling pathway activation of transformed cells. **A,** Self-renewal capacity of luminal A, luminal-like, normal-like, or basal-like transformed cell lines were measured by mammosphere assay. Primary mammospheres of SV40-T/t antigens ± *H-Ras*^{G12V} transformed basal-like cell line were more efficient than other cells in generating tertiary mammospheres. **B,** Mammosphere forming efficiency of luminal A, luminal-like, normal-like, or basal-like transformed cell lines. SV40-T/t antigens but not *H-Ras*^{G12V} increased the number of mammospheres. Asterisks denote significant differences compared with immortalized cell line. **C,** Cell-of-origin as well as oncogenes have an influence on the levels of stem/basal, progenitor, and differentiated cells in the mammospheres based on CD49f/EpCAM staining pattern. Red arrows indicate transformation-induced changes in phenotype of cells in mammospheres. **D,** Cell-of-origin as well as oncogenes have an influence on the levels of cancer stem-like cells (CD44$^+$/CD24$^-$) in mammospheres based on CD44/CD24 staining pattern. Red arrows indicate transformation-induced changes in phenotype of cells in mammospheres. **E,** pAKT (Ser473) and pSTAT3 (Tyr705) but not pERK (Thr202/Tyr204) and PTEN levels showed cell type and/or oncogene-dependent variability. SV40-T/t antigens reduced pAKT in luminal A and luminal-like but not in normal-like or basal cell line. Also note differences in basal pSTAT3 levels in control pLKO cells. **F,** BRD4, involved in epigenetic gene regulation and a drug target, shows cell type as well as oncogene-dependent changes in expression. Arrows show long and short isoforms.

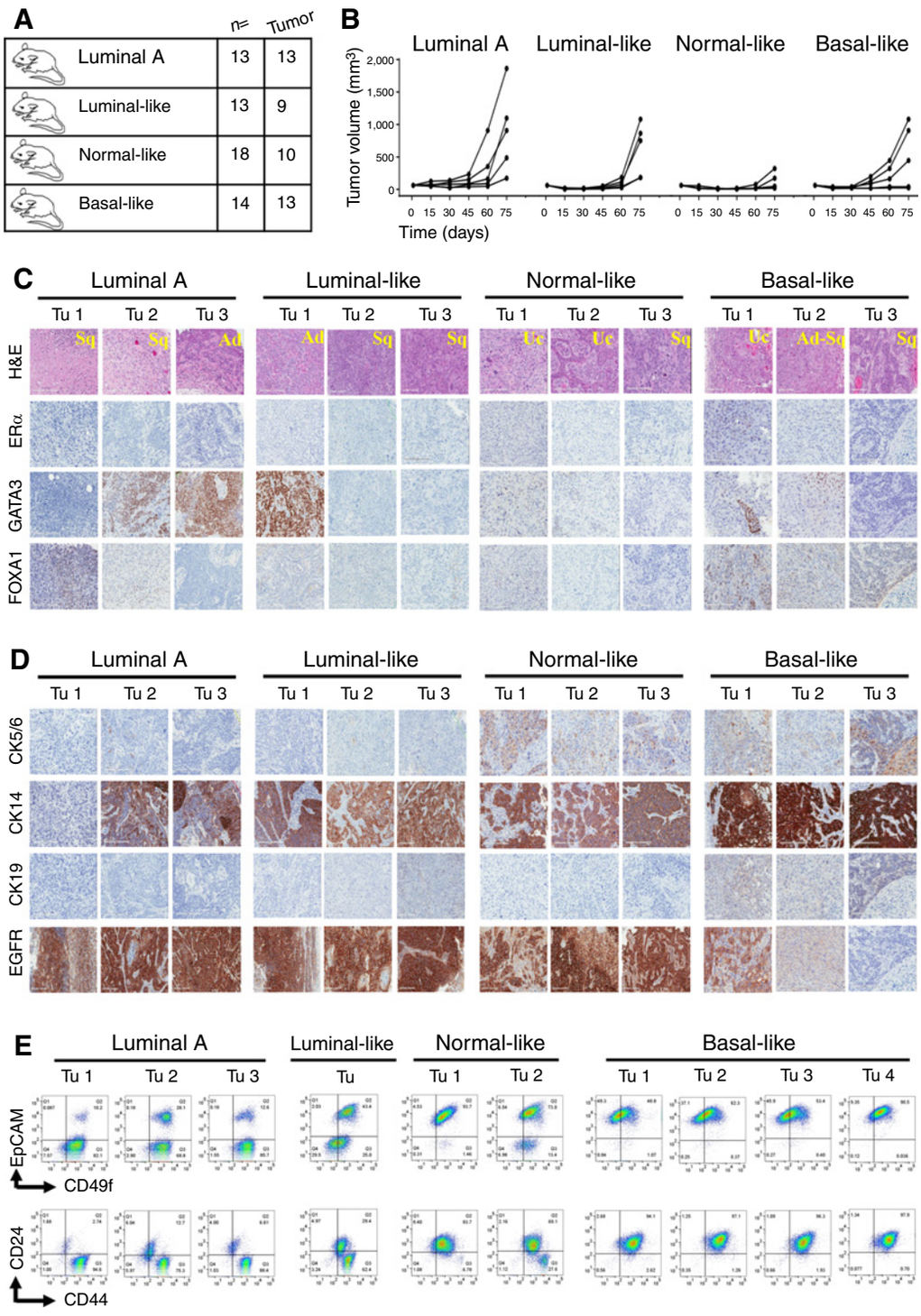

Figure 3.

Frequency and characteristics of tumors developed from *H-Ras*^{G12V}+ SV40-T/t transformed luminal A, luminal-like, normal-like, and basal-like cell lines. **A,** Tumor incidence by individual cell type transformed with *H-Ras*^{G12V}+ SV40-T/t. *N* corresponds to number of animals injected. **B,** Growth rate of tumors. **C,** Expression levels of luminal markers ERα, GATA3, and FOXA1 in tumors. H&E staining classified tumors as adenocarcinomas (Ad), squamous carcinoma (Sq), undifferentiated carcinomas (Uc), adenosquamous carcinoma (Ad-sq). **D,** Expression levels of cytokeratin CK5/6, CK14, CK19 and EGFR in tumors. Tumors derived from normal-like and basal-like expressed CK5/6. **E,** Cell lines derived from tumors of luminal A, luminal-like, normal-like, and basal-like double transformed cells were characterized by flow cytometry using CD49f/EpCAM and CD44/CD24 markers to determine stem/luminal progenitor/mature luminal cell hierarchy (CD49f/EpCAM) and cancer stem cell (CD44^{+}/CD24^{-}) properties.

positivity of many of these tumors, despite expressing luminal markers such as GATA3 and FOXA1, suggests that tumors represent recently modified intrinsic subtypes of breast cancers—myoluminal and myobasal subtypes (31, 32). Tumor derived from *H-Ras*^{G12V} transformed basal-like cells was CK5/6^{-}/CK14^{+}/CK19^{-} (Supplementary Fig. S3D). Tumors derived from each cell subtype were negative for CK8 expression (Supplementary Fig. S3D and S3E). Taken together, IHC analysis of ERα, GATA3, FOXA1, CK5/6, CK14, and CK19 again confirmed the intertumor heterogeneity, which could be due to differences in cell-of-origin of tumors.

Tumors derived from luminal A and luminal-like transformed cells display phenotypic heterogeneity

Because each cell lines generated distinct subtypes of tumors, we further characterized cell lines established from tumors for phenotypic heterogeneity. Cell lines were established after sorting human cells from mouse xenografts by flow cytometry using CD298 marker (Supplementary Fig. S3F). Cell lines established from tumors of luminal A-*H-Ras*^{G12V}+SV40-T/t transformed cells or luminal-like–*H-Ras*^{G12V}+SV40-T/t transformed cells contained morphologically distinct subpopulation of cells, whereas those derived from normal-like and basal-like cell lines were similar to parental cell lines (Supplementary Fig. S4A). Tumor-derived cell lines retained the expression of both mutant *Ras* and SV40-T/t antigens (Supplementary Fig. S4B). Tumor-derived cell lines of luminal A-*H-Ras*^{G12V}+SV40-T/t transformed cells showed two distinct subpopulations: CD49f^{+}/EpCAM^{-} and CD49f^{+}/EpCAM^{+}; CD44^{+}/CD24^{-} and CD44^{+}/CD24^{+}; CD201^{+}/EpCAM^{-} and CD201^{+}/EpCAM^{+}; and CD271$^{+/low}$/EpCAM^{-} and CD271$^{+/low}$/EpCAM^{+} cells (**Fig. 3E**; Supplementary Fig. S4C). These results indicate that there is acquired plasticity or clonal selection of transformed cells *in vivo* as the majority of transformed cells gained CD201 expression or CD201^{+} transformed cells were selected *in vivo*. Note that transformed luminal A cell line *in vitro* contained very low number of CD201^{+}/EpCAM^{-} cells (Supplementary Fig. S1C). In contrast to luminal A and luminal-like tumor-derived cell lines, normal-like and basal-like tumor-derived cells displayed one dominant population of cells, which were CD49f^{+}/EpCAM^{+}, CD44^{+}/CD24^{+}, CD201^{+}/EpCAM^{+} or CD271^{low}/EpCAM^{+} (**Fig. 3E**; Supplementary Fig. S4C). Thus, despite the same oncogenic mutations, cell-of-origin of transformed cells determine cancer stem cell and/or differentiation properties *in vivo*.

Because luminal A and luminal-like cell tumor-derived cell lines contained phenotypically distinct population of cells and to further rule out the possibility of any contaminating mouse cells, we used JAM-A and EpCAM to sort JAM-A^{+}/EpCAM^{+} and JAM-A^{-}/EpCAM^{-} subpopulation of cells and propagated these cells for further characterization. JAM-A has previously been shown to be expressed in glioma stem but not in normal brain cells and we had demonstrated its expression in breast epithelial cells (33, 34). JAM-A^{+}/EpCAM^{+} cells displayed cuboidal morphology, whereas JAM-A^{-}/EpCAM^{-} cells displayed spindle morphology (Supplementary Fig. S4D). Both population of cells expressed SV40-T antigen and *H-Ras*^{G12V} confirming that these cells are derived from original transplanted breast epithelial cells (Supplementary Fig. S4E). JAM-A^{+}/EpCAM^{+} cells were CD49f^{+}/EpCAM^{+}, CD44^{+}/CD24^{+}, CD201^{-}/EpCAM^{+}, CD201^{+}/EpCAM^{+} and CD271^{low}/EpCAM^{+} (Supplementary Fig. S4F). In contrast, JAM-A^{-}/EpCAM^{-} cells were CD49f^{+}/EpCAM^{-}, CD44^{+}/CD24^{-}, CD201^{+}/EpCAM^{-} and CD271^{low}/EpCAM^{-}. While the phenotype of JAM-A^{+}/EpCAM^{+} cells were similar to that of *in vitro* transformed cells, JAM-A^{-}/EpCAM^{-} phenotype was acquired by transformed cells *in vivo*. Note that oncogene-activated signaling pathways in tumor-derived cells and their *in vitro* counterparts were similar from all four cell types (Supplementary Fig. S4G–S4J).

Single cell-derived luminal A and luminal-like transformed cells display phenotypic heterogeneity

Phenotypic heterogeneity noted above in tumor-derived cell lines could be due to heterogeneity in immortalized cell lines from which transformed cells originated or due to acquired plasticity of transformed cells *in vivo*. To distinguish between these possibilities, we used soft agar assay to isolate single cell-derived tumorigenic clones. Tumor-derived cells from luminal A–*H-Ras*^{G12V}+SV40T/t, luminal-like–*H-Ras*^{G12V}+SV40T/t, and basal-like–*H-Ras*^{G12V}+SV40T/t transformed cells generated soft agar clones (**Fig. 4A**). Cells from tumor of normal-like–*H-Ras*^{G12V}+SV40T/t transformed cells formed smaller colonies. We next established two-dimensional (2D) cultures of these soft agar clones and confirmed SV40-T/t antigens and mutant *H-Ras*^{G12V} expression (**Fig. 4B**). Tumor cell lines derived from soft agar clones showed morphologic changes with aggressive phenotype such as limited cell–cell adhesion and spindle shape compared with parental cells (Supplementary Fig. S5A). These results suggest that anchorage-independent growth enforced by soft agar assay selects for transformed cells that have limited cell–cell adhesion properties.

To further characterize these clones for stem/luminal progenitor/mature luminal cell and cancer stem cell phenotypes, we performed flow cytometry with CD49f, EpCAM, CD44, and CD24 surface markers. The majority of clones contained cells that were CD49f^{+}/EpCAM^{-} and CD44^{+}/CD24^{-}, suggesting preferential growth of tumor cells with cancer stem cell properties in soft agar assay (**Fig. 4C**; Supplementary Fig. S5B). However, clone 6 of tumor 1, clones 3 and 6 of tumor 2 and clones 2, 4, and 5 of tumor 3 (luminal A-derived) contained a subpopulation of cells that were CD49f+/EpCAM+ and CD44+/CD24+ suggesting clonal differences in plasticity (**Fig. 4C**; Supplementary Fig. S5B). Cell surface staining patterns with isotype control antibodies are shown in Supplementary Fig. S5C, which were used for gating and to determine quadrants.

Interestingly, those clones with two different population of cells were also morphologically heterogeneous in 2D culture with both spindle and cuboidal cells (Supplementary Fig. S5A). Thus, it is likely that cell-of-origin determines plasticity of transformed cells.

To determine whether soft agar clones derived from luminal A–*H-Ras*^{G12V}+SV40T/t tumor cells form tumors of specific histotype, we injected 5×10^{6} cells from tumor 1 clone 6 (prominent CD49f^{+}/EpCAM^{-} subpopulations) and tumor 2 clone 6 (predominant CD49f^{+}/EpCAM^{+} subpopulation). CD49f^{+}/EpCAM^{-} cell-derived tumors were undifferentiated carcinomas, whereas tumors from CD49f^{+}/EpCAM^{+} cells were carcinomas (**Fig. 4D**). Tumors in both cases metastasized to lungs (**Fig. 4D**). Tumor developed from prominent CD49f^{+}/EpCAM^{-} subpopulation contained a small fraction of cells that were GATA3^{+}, whereas tumor and metastasis developed from CD49f^{+}/EpCAM^{+} cells showed strong GATA3 positivity (**Fig. 4D**).

Metastatic properties are governed by both cell-context and oncogenes

We next examined the relationship between cell context and oncogenes in metastatic progression. All luminal A–*H-Ras*^{G12V}+SV40-T/t, luminal-like–*H-Ras*^{G12V}+SV40-T/t and two of three basal-like–*H-Ras*^{G12V}+SV40-T/t cell-derived tumors showed metastasis to lungs, whereas none of the normal-like–*H-Ras*^{G12V}+SV40-T/t cells-derived tumors showed lung metastasis (**Fig. 5A** and **B**). Lung metastasis expressed GATA3 but not FOXA1 in luminal A and luminal-like cells-derived tumors. Interestingly, lung

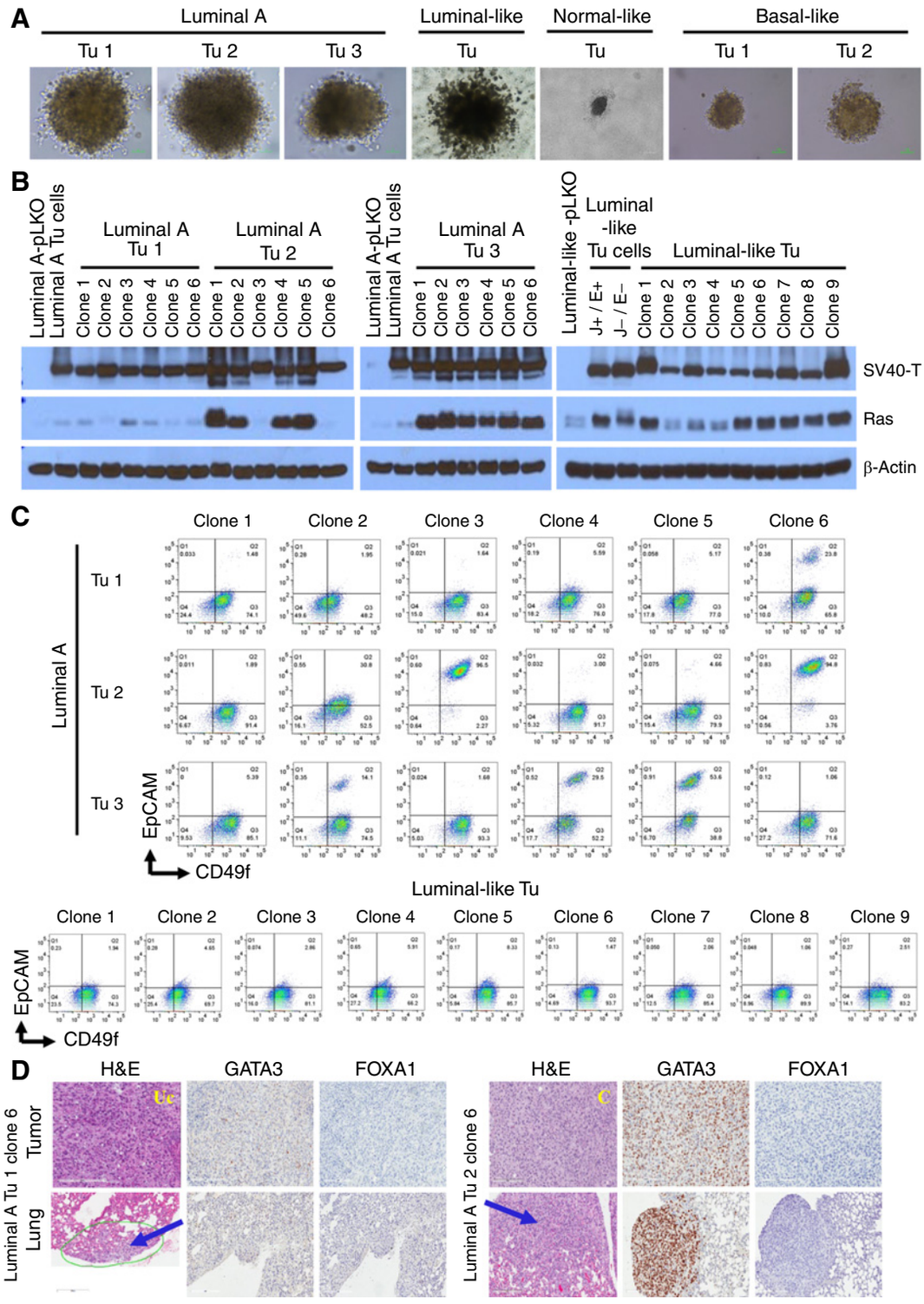

Figure 4.

Single cell-derived tumor cells generate metastatic tumors. **A,** Isolation of individual tumor cell-derived cell lines using soft agar assay. Soft agar colonies from various tumor-derived cell lines are shown. **B,** SV40-T antigen and *H-Ras*^{G12V} expression in soft agar colony-derived cell lines. β-actin was used as an internal control. **C,** The majority of cells in soft agar clones-derived cell lines are enriched for CD49f^{+}/EpCAM^{-} stem cell markers. **D,** Tumor developed from the soft agar clones of luminal A tumor cells (cell lines with prominent CD49f^{+}/EpCAM^{-} cells, left, and CD49f^{+}/EpCAM^{+} cells, right) metastasized to lungs. The expressions of GATA3 and FOXA1 were analyzed in tumors and lungs metastasis by immunohistochemistry. Representative IHC data are shown.

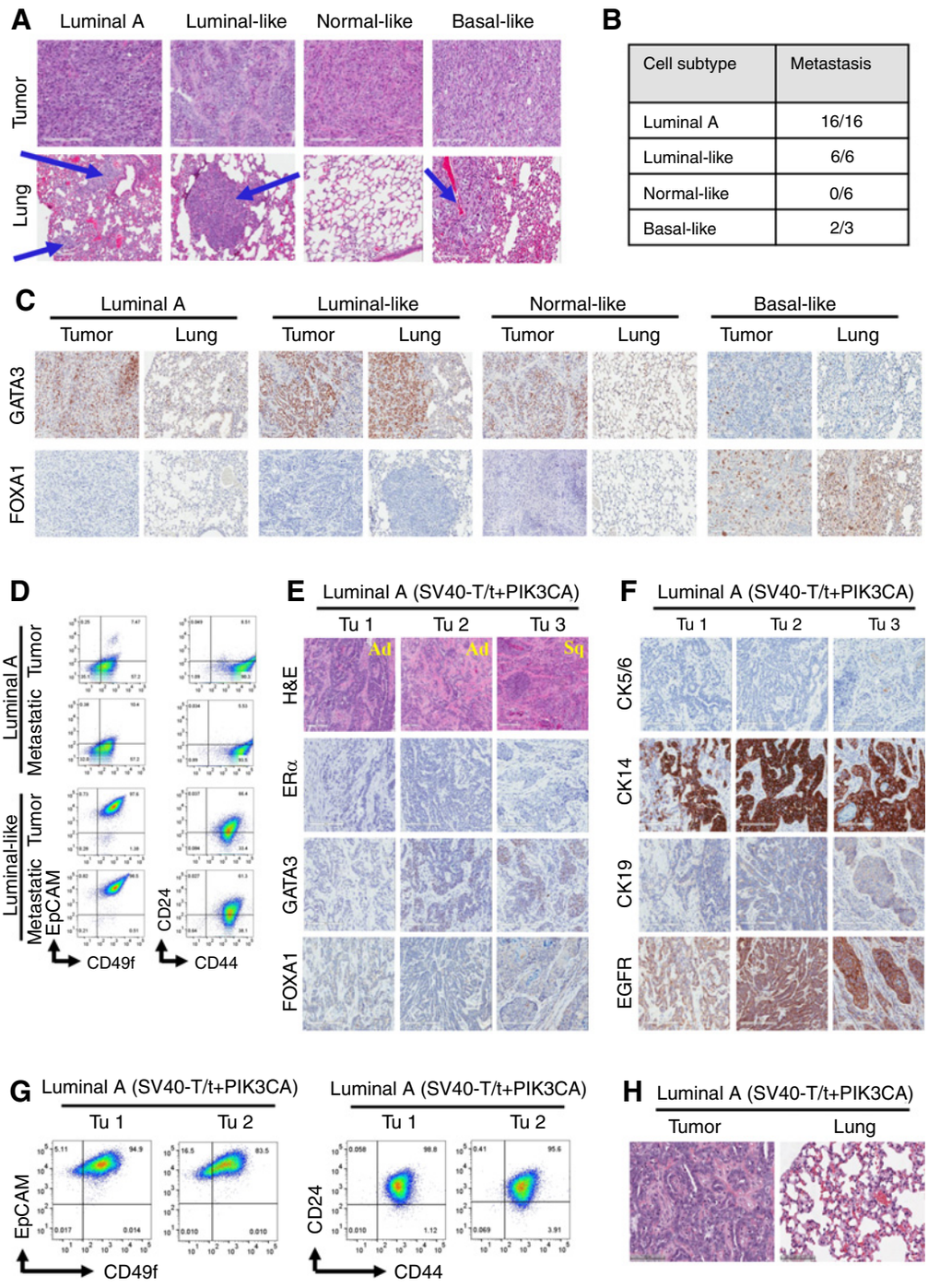

Cell subtype	Metastasis
Luminal A	16/16
Luminal-like	6/6
Normal-like	0/6
Basal-like	2/3

Figure 5.

Bidirectional cross-talk between cell-context and oncogenes determine metastatic properties. **A,** H&E staining shows tumors developed from the luminal A, luminal-like, and basal-like but not normal-like double transformed cell lines metastasize to lungs. **B,** Frequency of metastasis of luminal A, luminal-like, normal-like, and basal-like cell-derived tumors. **C,** Expression levels of GATA3 and FOXA1 in tumors and lung metastasis. **D,** Cells derived from tumors and lung metastasis of luminal A and luminal-like double transformed cells were characterized by flow cytometry using CD49f/EpCAM and CD44/CD24 markers to determine stem/luminal progenitor/mature luminal properties and cancer stem cell phenotype. **E,** Histotype and expression levels of luminal markers ERα, GATA3, and FOXA1 in tumors developed from luminal A cells double transformed with SV40-T/t and *PIK3CA* (luminal A-SV40-T/t + *PIK3CA* cells). **F,** Expression levels of cytokeratin CK5/6, CK14, CK19 and EGFR in tumors developed from luminal A-SV40-T/t + *PIK3CA* cells. **G,** Unlike cells from SV40-T/t + *H-Ras*^{G12V}-derived tumors, cells derived from tumors of luminal A-SV40-T/t + *PIK3CA* were not enriched for CD49f^{+}/EpCAM^{-} stem cells or CD44^{+}/CD24^{-} cancer stem cells. **H,** Tumors derived from luminal A-SV40-T/t + *PIK3CA* transformed cells fail to metastasize to lungs.

metastasis of basal-like–derived tumors expressed luminal markers FOXA1 and contained few GATA3+ cells, suggesting that tumor and lung metastasis in basal-like cell lines originated from a small fraction of luminal-like cells within the basal-like cell line (**Fig. 5C**).

Cell lines were created from matched tumors and metastasis to determine whether metastatic cells acquire additional phenotype compared with primary tumor cells (**Fig. 5D**; Supplementary Fig. S6A and S6B). Luminal A–*H-Ras*^{G12V}+SV40T/t tumor and metastatic cells showed similar staining patterns, that is, CD49f$^{+/low}$/EpCAM^{-}, CD44^{+}/CD24^{-}, CD201^{+}/EpCAM^{-}, and CD271^{low}/EpCAM^{-} (**Fig. 5D**; Supplementary Fig. S6B). Similar results were obtained with luminal-like–*H-Ras*^{G12V}+SV40T/t tumor and metastatic cells, that is, CD49f^{+}/EpCAM^{+}, CD44^{+}/CD24^{-}, CD44^{+}/CD24^{+}, CD201^{+}/EpCAM^{-}, CD201^{+}/EpCAM^{+}, CD271^{-}/EpCAM^{+} and CD271^{+}/EpCAM^{+} (**Fig. 5D**; Supplementary Fig. S6B). Thus, at least phenotypically, primary and metastatic cells are similar.

To determine the role of oncogenes in metastatic phenotype, we created a new series of cell lines that overexpressed breast cancer relevant mutant *PIK3CA* and SV40-T/t antigens. Luminal A and normal-like cells were transformed with either mutant *PIK3CA* (*PIK3CA*^{H1047R}) alone or a combination of SV40-T/t antigens and *PIK3CA*^{H1047R} (Supplementary Fig. S6C). The normal-like cells transformed with *PIK3CA*^{H1047R} alone or in combination with SV40-T/t antigens did not form tumor. Luminal A cells transformed with *PIK3CA*^{H1047R} alone did not form tumor, but in combination with SV40-T/t antigens formed tumors. Luminal A-SV40T/t+*PIK3CA*^{H1047R} transformed cell-derived tumors were adenocarcinoma and poorly differentiated squamous cell carcinoma (**Fig. 5E**). Staining of tumors developed from luminal A-SV40T/t+*PIK3CA*^{H1047R} transformed cells showed both ERα^{-}/GATA3^{+}/FOXA1^{+} and ERα^{-}/GATA3^{-}/FOXA1^{-} subpopulations (**Fig. 5E**). Keratins expression profiles of tumors were CK5/6^{-}/CK14^{+} with a small population of CK19^{+} cells and all the tumors were EGFR^{+} (**Fig. 5F**).

Cell lines were established after sorting human cells from mouse xenografts of luminal A-SV40T/t+*PIK3CA*^{H1047R} transformed cells using CD298 marker (Supplementary Fig. S6D). Tumor-derived cell lines of luminal A-SV40T/t+*PIK3CA*^{H1047R} transformed cells displayed CD49f^{+}/EpCAM^{+} and CD49f^{-}/EpCAM^{+}; CD44^{+}/CD24^{+}; CD201^{+}/EpCAM^{+} and CD201^{-}/EpCAM^{+}; and CD271^{-}/EpCAM^{+} and CD271^{+}/EpCAM^{+} phenotypes and minimally enriched for cells with cancer stem cell phenotype (**Fig. 5G**; Supplementary Fig. S6E) compared with luminal A-*H-Ras*^{G12V}+SV40T/t transformed cells (See **Fig. 3E**; Supplementary Fig. S4C). None of the luminal A-SV40T/t+*PIK3CA*^{H1047R} cell-derived tumors metastasized to lungs (**Fig. 5H**), whereas luminal A–*H-Ras*^{G12V}+SV40T/t cell-derived tumors showed metastasis to lung (see **Fig. 5A** and **B**). These results suggest that a bidirectional regulatory relationship between cell-context and oncogenes determine acquisition of cancer stem cell phenotype and metastasis properties *in vivo*.

Oncogenes, irrespective of cell context, determine susceptibility to DNA-damaging agents

To understand whether bidirectional relationship between cell-context and oncogenes extend to response to chemotherapy, we determined double-stranded DNA break (DSB) response of immortalized and transformed cells upon treatment with chemotherapeutic agents. Flow cytometry was used to identify induction of an established marker for unrepaired DSBs γ-H2AX in response to 48 hours of treatment with doxorubicin, paclitaxel, and cisplatin (35). The type of oncogene instead of cell context of transformed cells influenced DSB response, as doxorubicin increased γ-H2AX levels more efficiently in SV40-T/t antigens overexpressing cells compared with *H-Ras*^{G12V}-overexpressing cells (**Fig. 6A**). Similar effects were observed with paclitaxel (**Fig. 6B**) and cisplatin treatment (**Fig. 6C**). However, *H-Ras*^{G12V} dominantly reduced DSB response because γ-H2AX levels were lower in double-transformed cells compared with SV40-T/t transformed cells.

To further investigate oncogene-dependent changes in DSB response and potential resolution of DSB, we performed co-localization studies of γ-H2AX and RAD51. Co-localization of these two molecules indicates active repair of DSBs (36). Doxorubicin-treated pLKO and *H-Ras*^{G12V} transformed cells showed strong γ-H2AX and RAD51 co-localization and distinct foci, whereas signals in SV40-T/t antigens transformed cells were much more diffuse (**Fig. 6D**). Taken together, these results indicate that while DNA repair pathways are relatively unaffected in pLKO and *H-Ras*^{G12V} transformed cells, SV40-T/t antigens induced signals disrupt DNA repair.

Therapy-induced apoptosis is oncogene dependent

To elucidate the role of oncogenes in chemotherapy-induced apoptosis, Annexin V staining was performed to measure response to doxorubicin, paclitaxel, and cisplatin. SV40-T/t antigens transformed cells compared with immortalized pLKO or *H-Ras*^{G12V} transformed cells were more sensitive to doxorubicin-, paclitaxel-, and cisplatin-induced apoptosis (**Fig. 7A–D**). Colony formation assay was used to further confirm oncogene-dependent susceptibility of transformed cells to chemotherapy. As with other two assays, SV40-T/t antigens transformed cells were more sensitive to doxorubicin and showed reduced number of colonies compared with immortalized or *H-Ras*^{G12V} transformed cells (Supplementary Fig. S7A and S7B).

Isogenic cell line resource to study the interplay between cell-of-origin and oncogenes on various facets of cancer progression

During the course of this investigation, we have created an important resource for research community to further investigate interplay between cell-of-origin and defined oncogenes in cancer progression. These cell lines are suitable to study cell context–dependent oncogene-induced epigenomic changes under the same genetic background. Phenotype and genetic ancestry of these cell lines are described in Supplementary Table S1. Because transformed variants of several of these cell lines spontaneously metastasize to lungs, these cell lines are useful for screening of drugs that not only target primary tumors but also metastasis.

Discussion

Tumor heterogeneity has a serious clinical consequence as it contributes to drug resistance, metastatic spread, and even improper molecular classification of cancer that affect treatment decision making (37). It is believed that tumor heterogeneity has at least three origins; pliancy of initially transformed cell (cell-of-origin), adaptive plasticity of transformed cells, and genomic aberrations (37, 38). Although multiple breast cancer subtypes including basal type are suggested to originate from luminal progenitor cells (5, 6), the most susceptible population within the heterogenous population of luminal cells are yet to be identified and experimentally analyzed. The majority of transformation assays of breast epithelial cells gave rise to squamous carcinomas (39). The adenocarcinoma phenotype has been hard to

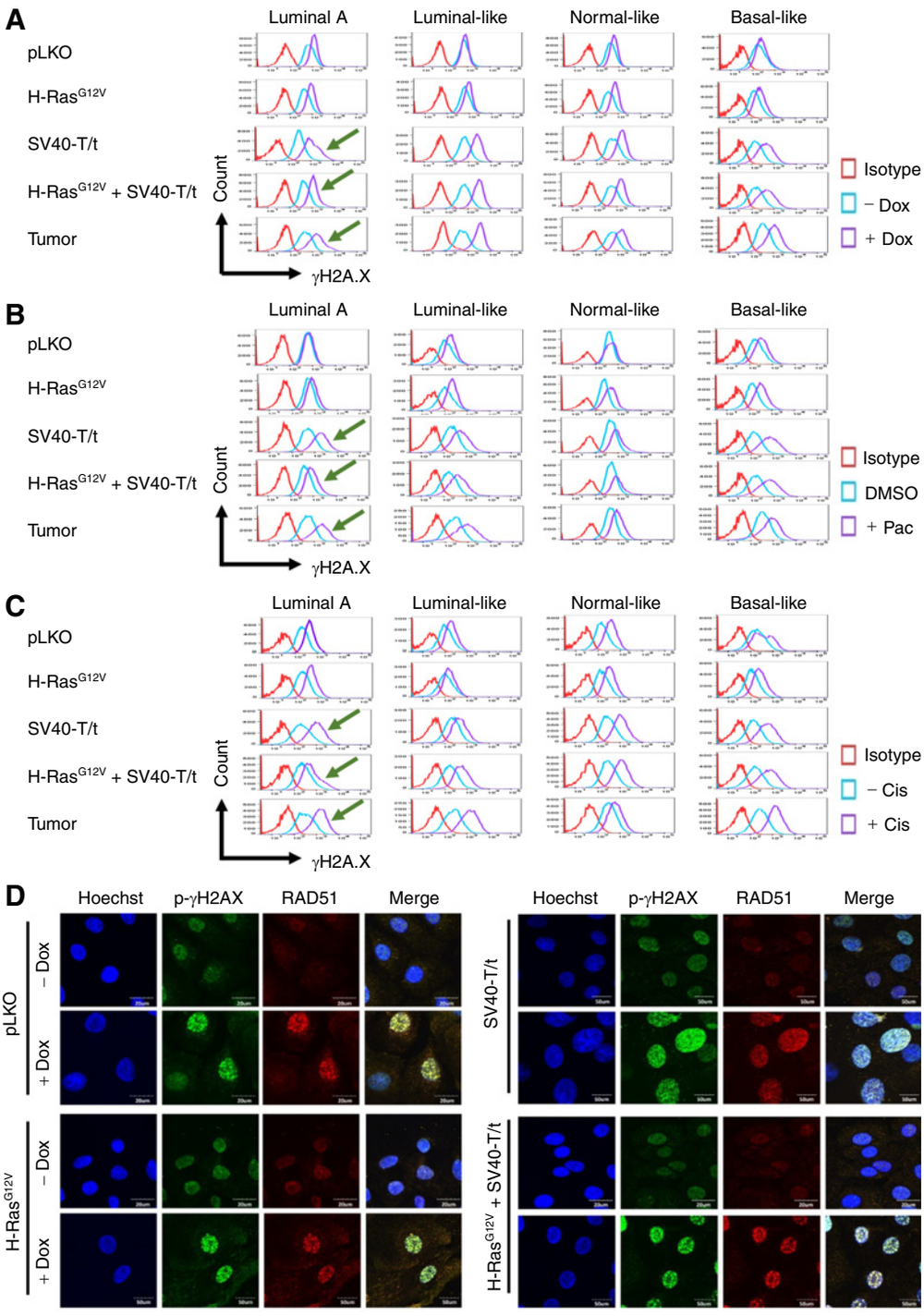

Figure 6.

Oncogenes determine susceptibility to DNA-damaging agents independent of cell-of-origin of transformation. **A,** DSB response in luminal A, luminal-like, normal-like, and basal-like immortalized, transformed, and tumor cells was examined after treatment with doxorubicin (Dox, 250 nmol/L for 48 hours) by flow cytometry using pγ-H2AX as a marker. **B,** DSB response in luminal A, luminal-like, normal-like, and basal-like immortalized, transformed, and tumor cells was examined after treatment with paclitaxel (Pac, 100 nmol/L for 48 hours) by flow cytometry using pγ-H2AX. **C,** Same assay as in **A** and **B** except that cells were treated with 5 μmol/L cisplatin for 48 hours. **D,** Immunofluorescence staining with pγ-H2AX and RAD51 antibodies was used to measure the response to doxorubicin. Recruitment of RAD51 to pγ-H2AX–positive foci indicating repair of damaged DNA is evident in pLKO and *H-Ras^{G12V}* transformed cells but not in SV40-T/t antigen expressing cells. *H-Ras^{G12V}* restores repair process as higher levels of pγ-H2AX and RAD51 co-localization was observed in double transformed cells compared with SV40-T/t transformed cells.

Q6

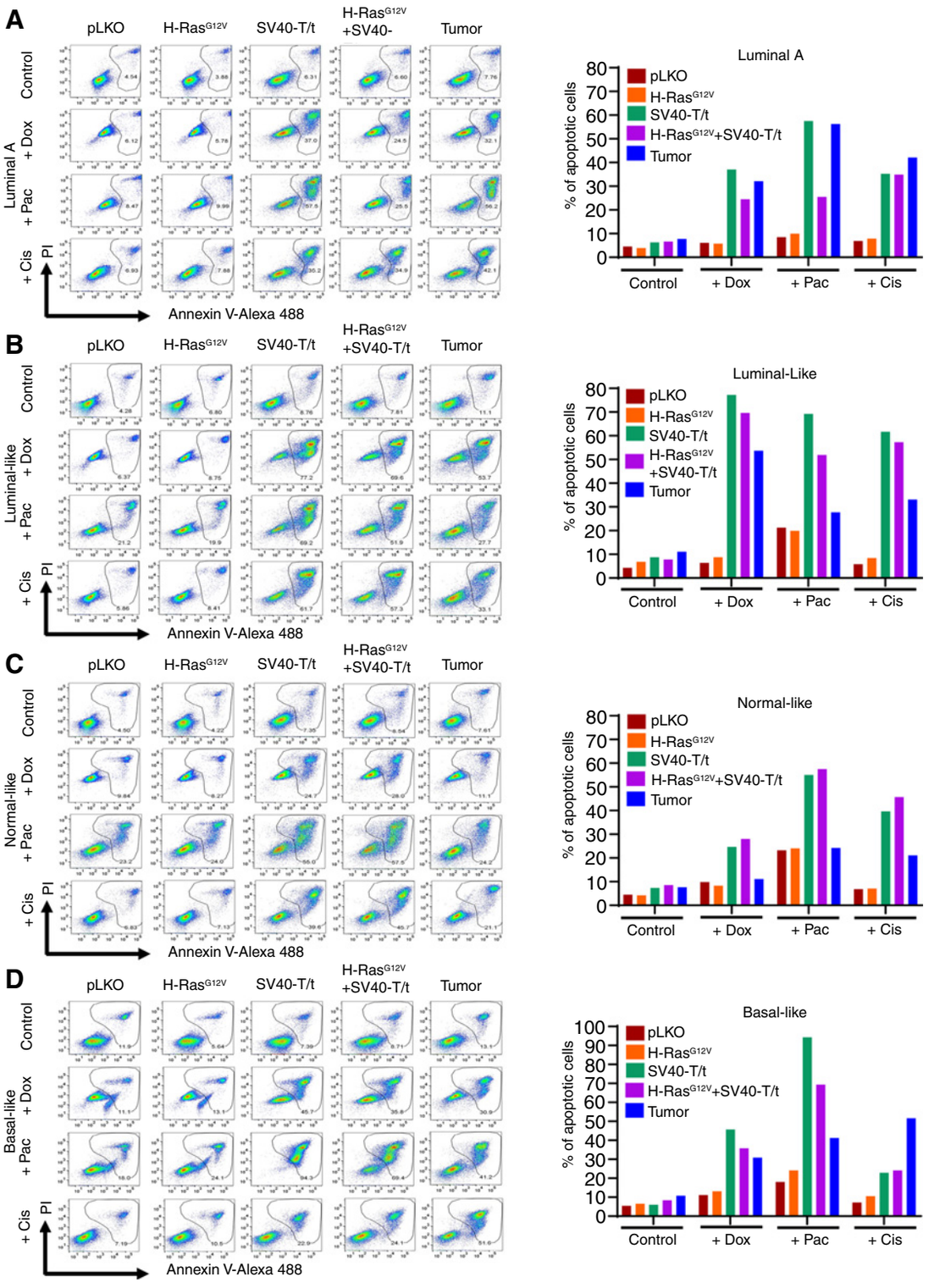

Figure 7.

Therapy-induced apoptosis is oncogene-dependent. Annexin V staining was used to measure response to chemotherapeutic drugs doxorubicin, paclitaxel, and cisplatin. Percentage of Annexin V ± PI positive cells under various conditions are shown on the right. **A,** Luminal A immortalized, transformed, and primary tumor-derived cells. **B,** Luminal-like immortalized, transformed, and primary tumor-derived cells. **C,** Normal-like immortalized, transformed, and primary tumor-derived cells. **D,** Basal-like immortalized, transformed, and primary tumor-derived cells. **Visual Overview:** A schematic diagram representing the flow of the study.

Q7

recapitulate in *in vivo* tumor models (40, 41), although this tumor histotype comprises the majority of tumors naturally occurring in breast and other cancers (42). Ince and colleagues, have shown that the same set of oncogenes can generate metastatic adenocarcinomas or non-metastatic squamous carcinomas depending on growth media used for initial isolation/propagation of cells, which provided first indication to cell-of-origin determining histotype of tumors (12). Previous studies in this respect had a major limitation as breast epithelial cell lines used were derived from reduction mammoplasty samples or normal tissues adjacent to tumors with aberrant genomes, which we and others have shown them to be molecularly/histologically abnormal (43–45). Here, we used the cell lines derived from biopsies of healthy donors of different genetic ancestry to develop an assay system that closely recapitulates naturally occurring human breast cancer, including their metastatic behavior. As we reported previously, these cell lines remained diploid when we tested them at approximately 20 passage (18). The use of reduction mammaplasty samples instead of normal breast epithelial cells could be a reason for discrepancy between data presented here and by Nguyen and colleagues, (10). Authors using purified luminal progenitors ($CD49f^{+}/EpCAM^{+}$) and basal cells ($CD49f^{+}/EpCAM^{-}$) and activated *K-Ras*^{G12D} oncogene suggested that potent oncogenic role of this oncogene rather than the epithelial cell type of the breast determines histopathology of resulting tumors. Our study, however, suggests the role of cell-of-origin in determining histopathology of tumors.

Cell line models used here allowed us systematic analyses that could address the following questions: (i) Can we achieve transformation of breast epithelial cells derived from healthy donors using a single oncogene or need more than one oncogene?; (ii) Instead of one "normal" cell line typically used in the literature to understand the signaling axis downstream of oncogenic activation, do breast epithelial cell lines derived from multiple donors reveal similar downstream signaling by an oncogene?; (iii) Will the use of multiple cell lines allow us to dissect the roles of cell-of-origin and oncogenic mutations on various steps of the oncogenic processes including acquiring cancer stem cell phenotype, metastasis patterns, and response to therapy?; and (iv) do cells enriched for luminal and basal cell gene expression patterns differ in their susceptibility to transformation? Our results suggest that cell-of-origin determines histology of tumors as only cells enriched for luminal epithelial gene expression patterns gave rise to adenocarcinomas, whereas all tumors originating from cells with basal or normal-like intrinsic breast cancer subtype gene expression rarely generated adenocarcinoma. While *H-Ras*^{G12V} alone was able to transform basal-like cell line at a very low frequency, luminal-like cell lines required two oncogenes (*H-Ras*^{G12V} or *PIK3CA*^{H1047R} and SV40-T/t). Thus, cell-of-origin also determines requirement of oncogenes for transformation. It is unclear at present which among known downstream targets of SV40-T/t antigens [RB, p53, PP2A, or p16 inactivation (46)] is essential or sufficient along with *H-Ras*^{G12V} or *PIK3CA*^{H1047R} for transformation. Further studies are required in this direction.

Signaling pathway activation in transformed cells is dependent on bidirectional interaction between cell context and oncogenes. For example, SV40-T/t antigens reduced pAKT in luminal-like cell lines but not in basal- or normal-like cell lines. SV40-T/t antigens induced NFκB DNA binding more robustly in the normal-like cell line compared with luminal-like cell lines. *H-Ras*^{G12V} but not SV40-T/t antigens had cell type–specific effects on BRD4 induction. These cell type–specific effects of oncogenes in inducing signaling pathways may be a reason for lack of uniform activity of drugs that target signaling pathways downstream of oncogenes. Also, oncogene-induced increase in BRD4 levels correlated with lower response to JQ1. Thus, an interplay between oncogenic aberrations and cell-of-origin of tumor may determine sensitivity to targeted therapies such as JQ1, which is often difficult to discern from genomic analyses of tumors.

We observed that bidirectional interaction between cell-context and oncogenic signals additionally determine clonal diversity, cancer stem cell phenotype, and metastasis patterns. For example, SV40-T/t antigens overexpression resulted in significant phenotypic diversity only in luminal A and basal-like cell lines but not in normal-like cell line while *H-Ras*^{G12V} did not cause phenotypic diversity in any cell lines. *In vivo*, luminal A and luminal-derived tumors but not tumors derived from normal or basal-like cell lines gained $CD201^{+}/EpCAM^{-}$ phenotype. While both luminal and basal-like cell lines transformed with *H-Ras*^{G12V} plus SV40-T/t antigens developed metastatic tumors, luminal cell lines transformed with *PIK3CA*^{H1047R} plus SV40-T/t antigens developed only non-metastatic tumors. Clearly, interactions between genomic aberrations and potentially the epigenome of the cell types are required for cancer cells to acquire metastatic properties. A systematic epigenome, transcriptome, and proteome analysis of isogenic cell line models listed in Supplementary Table S1 may be essential to reveal complex interplay between cell-context and genomic aberrations.

Only property of tumor cells that is independent of cell-of-origin is the response to chemotherapeutic agents. SV40-T/t antigens overexpressing but not *H-Ras*^{G12V}-overexpressing cells were sensitive to all three drugs that we have tested in multiple assays. Mechanisms behind their sensitivity are unknown but further exploration may yield important clues to mechanisms of chemotherapeutic resistance.

In conclusion, using unique set of immortalized luminal A, luminal-like, normal-like, and basal-like cell lines generated using breast biopsies of healthy women, we have created a model system to study the effects of cellular pliancy and genomic aberrations on various steps of cancer progression. Visual overview provides a synapsis our findings. Our studies clearly indicate the need to use multiple "normal" cell line resources to understand interplay between cell type and genomic aberrations as well as for identifying universally activated signaling pathway downstream of a genomic aberration, which is critical for developing targeted therapies. These unique cell line models will be highly useful in understanding the mechanisms that contribute to tumor heterogeneity, developmental hierarchy for breast cancer cells, therapy resistance and may help to develop predictive markers of breast cancer metastasis in future.

Authors' Disclosures

G. Sandusky reports no other relationships. H. Nakshatri reports grants from Department of Defense, Susan G Komen for the Cure, 100 Voices of Hope, Breast Cancer Research Foundation, and Vera Bradley Foundation for Breast Cancer Research during the conduct of the study; grants from Department of Veterans Affairs, Chan-Zuckerberg Initiative, and NIH outside the submitted work. No disclosures were reported by the other authors.

Authors' Contributions

B. Kumar: Data curation, formal analysis, visualization, methodology, writing–original draft. **P. Bhat-Nakshatri:** Data curation, formal analysis, visualization, methodology. **C. Maguire:** Data curation, formal analysis, visualization. **M. Jacobsen:** Data curation, formal analysis, visualization. **C.J. Temm:** Formal analysis, visualization, methodology. **G. Sandusky:** Data curation, formal analysis, visualization, methodology. **H. Nakshatri:** Conceptualization, resources, data curation, formal analysis, supervision, funding acquisition, validation, investigation, methodology, writing–original draft, project administration, writing–review and editing.

Acknowledgments

We thank Connie J. Eaves (University of British Columbia, Vancouver, Canada) for mutant *PIK3CA* vector, members of the IUSCC flow cytometry core, confocal microscopy core, animal facility, and tissue procurement cores at the IU Simon Cancer center and Susan G Komen Tissue Bank for various tissues and reagents. We also thank countless number of women for donating their breast tissue for research purpose as well as volunteers who facilitated tissue collection. We also thank Rakesh Kumar for his suggestions to improve the article. This work is supported by DOD-W81XWH-15-1-0707, DOD-WH1XWH2010577, Susan G. Komen for the Cure (SAC110025) and 100 Voices of Hope to HN. Susan G. Komen for the Cure, Breast Cancer Research Foundation and Vera Bradley Foundation for Breast Cancer Research provide funding support to Komen Normal Tissue Bank.

The costs of publication of this article were defrayed in part by the payment of page charges. This article must therefore be hereby marked *advertisement* in accordance with 18 U.S.C. Section 1734 solely to indicate this fact.

Received March 5, 2021; revised June 2, 2021; accepted July 16, 2021; published first July 20, 2021.

References

1. Sorlie T, Perou CM, Tibshirani R, Aas T, Geisler S, Johnsen H, et al. Gene expression patterns of breast carcinomas distinguish tumor subclasses with clinical implications. Proc Natl Acad Sci U S A 2001;98: 10869–74.
2. Curtis C, Shah SP, Chin SF, Turashvili G, Rueda OM, Dunning MJ, et al. The genomic and transcriptomic architecture of 2,000 breast tumours reveals novel subgroups. Nature 2012;486:346–52.
3. Prat A, Perou CM. Mammary development meets cancer genomics. Nat Med 2009;15:842–4.
4. Fu NY, Rios AC, Pal B, Law CW, Jamieson P, Liu R, et al. Identification of quiescent and spatially restricted mammary stem cells that are hormone responsive. Nat Cell Biol 2017;19:164–76.
5. Proia TA, Keller PJ, Gupta PB, Klebba I, Jones AD, Sedic M, et al. Genetic predisposition directs breast cancer phenotype by dictating progenitor cell fate. Cell Stem Cell 2011;8:149–63.
6. Lim E, Vaillant F, Wu D, Forrest NC, Pal B, Hart AH, et al. Aberrant luminal progenitors as the candidate target population for basal tumor development in BRCA1 mutation carriers. Nat Med 2009;15:907–13.
7. Bhat-Nakshatri P, Gao P, Sheng L, McGuire PC, Xuei X, Wan J, et al. A single cell atlas of the healthy breast tissues reveals clinically relevant clusters of breast epithelial cells. Cell Rep Med 2021;2:100219.
8. Keller PJ, Lin AF, Arendt LM, Klebba I, Jones AD, Rudnick JA, et al. Mapping the cellular and molecular heterogeneity of normal and malignant breast tissues and cultured cell lines. Breast Cancer Res 2010;12:R87.
9. Keller PJ, Arendt LM, Skibinski A, Logvinenko T, Klebba I, Dong S, et al. Defining the cellular precursors to human breast cancer. Proc Natl Acad Sci U S A 2012;109:2772–7.
10. Nguyen LV, Pellacani D, Lefort S, Kannan N, Osako T, Makarem M, et al. Barcoding reveals complex clonal dynamics of de novo transformed human mammary cells. Nature 2015;528:267–71.
11. Cancer Genome Atlas Network. Comprehensive molecular portraits of human breast tumours. Nature 2012;490:61–70.
12. Ince TA, Richardson AL, Bell GW, Saitoh M, Godar S, Karnoub AE, et al. Transformation of different human breast epithelial cell types leads to distinct tumor phenotypes. Cancer Cell 2007;12:160–70.
13. Elenbaas B, Spirio L, Koerner F, Fleming MD, Zimonjic DB, Donaher JL, et al. Human breast cancer cells generated by oncogenic transformation of primary mammary epithelial cells. Genes Dev 2001;15:50–65.
14. Wright KL, Adams JR, Liu JC, Loch AJ, Wong RG, Jo CE, et al. Ras signaling is a key determinant for metastatic dissemination and poor survival of luminal breast cancer patients. Cancer Res 2015;75:4960–72.
15. Wander SA, Cohen O, Gong X, Johnson GN, Buendia-Buendia JE, Lloyd MR, et al. The genomic landscape of intrinsic and acquired resistance to cyclin-dependent kinase 4/6 inhibitors in patients with hormone receptor-positive metastatic breast cancer. Cancer Discov 2020;10:1174–93.
16. Hahn WC, Dessain SK, Brooks MW, King JE, Elenbaas B, Sabatini DM, et al. Enumeration of the simian virus 40 early region elements necessary for human cell transformation. Mol Cell Biol 2002;22:2111–23.
17. Deeb KK, Michalowska AM, Yoon CY, Krummey SM, Hoenerhoff MJ, Kavanaugh C, et al. Identification of an integrated SV40 T/t-antigen cancer signature in aggressive human breast, prostate, and lung carcinomas with poor prognosis. Cancer Res 2007;67:8065–80.
18. Kumar B, Prasad MS, Bhat-Nakshatri P, Anjanappa M, Kalra M, Marino N, et al. Normal breast-derived epithelial cells with luminal and intrinsic subtype-enriched gene expression document inter-individual differences in their differentiation cascade. Cancer Res 2018;78:5107–23.
19. Bhat-Nakshatri P, Sweeney CJ, Nakshatri H. Identification of signal transduction pathways involved in constitutive NF-kappaB activation in breast cancer cells. Oncogene 2002;21:2066–78.
20. Kumar S, Kishimoto H, Chua HL, Badve S, Miller KD, Bigsby RM, et al. Interleukin-1 alpha promotes tumor growth and cachexia in MCF-7 xenograft model of breast cancer. Am J Pathol 2003;163:2531–41.
21. Prasad M, Kumar B, Bhat-Nakshatri P, Anjanappa M, Sandusky G, Miller KD, et al. Dual TGFbeta/BMP pathway inhibition enables expansion and characterization of multiple epithelial cell types of the normal and cancerous breast. Mol Cancer Res 2019;17:1556–70.
22. Visvader JE, Stingl J. Mammary stem cells and the differentiation hierarchy: current status and perspectives. Genes Dev 2014;28:1143–58.
23. Wang D, Cai C, Dong X, Yu QC, Zhang XO, Yang L, et al. Identification of multipotent mammary stem cells by protein C receptor expression. Nature 2014; 517:81–4.
24. Kim J, Villadsen R, Sorlie T, Fogh L, Gronlund SZ, Fridriksdottir AJ, et al. Tumor initiating but differentiated luminal-like breast cancer cells are highly invasive in the absence of basal-like activity. Proc Natl Acad Sci U S A 2012;109:6124–9.
25. Al-Hajj M, Wicha MS, Benito-Hernandez A, Morrison SJ, Clarke MF. Prospective identification of tumorigenic breast cancer cells. Proc Natl Acad Sci U S A 2003;100:3983–8.
26. Carbognin L, Miglietta F, Paris I, Dieci MV. Prognostic and predictive implications of PTEN in breast cancer: unfulfilled promises but intriguing perspectives. Cancers 2019;11:1401.
27. Shu S, Polyak K. BET bromodomain proteins as cancer therapeutic targets. Cold Spring Harb Symp Quant Biol 2016;81:123–9.
28. Alsarraj J, Walker RC, Webster JD, Geiger TR, Crawford NP, Simpson RM, et al. Deletion of the proline-rich region of the murine metastasis susceptibility gene Brd4 promotes epithelial-to-mesenchymal transition- and stem cell-like conversion. Cancer Res 2011;71:3121–31.
29. Sahni JM, Keri RA. Targeting bromodomain and extraterminal proteins in breast cancer. Pharmacol Res 2018;129:156–76.
30. Lawson DA, Bhakta NR, Kessenbrock K, Prummel KD, Yu Y, Takai K, et al. Single-cell analysis reveals a stem-cell program in human metastatic breast cancer cells. Nature 2015;526:131–5.
31. Mathews JC, Nadeem S, Levine AJ, Pouryahya M, Deasy JO, Tannenbaum A. Robust and interpretable PAM50 reclassification exhibits survival advantage for myoepithelial and immune phenotypes. NPJ Breast Cancer 2019;5:30.
32. Roelands J, Mall R, Almeer H, Thomas R, Mohamed MG, Bedri S, et al. Ancestry-associated transcriptomic profiles of breast cancer in patients of African, Arab, and European ancestry. NPJ Breast Cancer 2021;7:10.
33. Lathia JD, Li M, Sinyuk M, Alvarado AG, Flavahan WA, Stoltz K, et al. High-throughput flow cytometry screening reveals a role for junctional adhesion molecule a as a cancer stem cell maintenance factor. Cell Rep 2014;6:117–29.
34. Nakshatri H, Anjanappa M, Bhat-Nakshatri P. Ethnicity-dependent and -independent heterogeneity in healthy normal breast hierarchy impacts tumor characterization. Sci Rep 2015;5:13526.
35. Mah LJ, El-Osta A, Karagiannis TC. gammaH2AX: a sensitive molecular marker of DNA damage and repair. Leukemia 2010;24:679–86.
36. Rothkamm K, Barnard S, Moquet J, Ellender M, Rana Z, Burdak-Rothkamm S. DNA damage foci: meaning and significance. Environ Mol Mutagen 2015;56: 491–504.
37. Yap TA, Gerlinger M, Futreal PA, Pusztai L, Swanton C. Intratumor heterogeneity: seeing the wood for the trees. Sci Transl Med 2012;4:127ps10.
38. Gupta PB, Pastushenko I, Skibinski A, Blanpain C, Kuperwasser C. Phenotypic plasticity: driver of cancer initiation, progression, and therapy resistance. Cell Stem Cell 2019;24:65–78.

39. Dimri G, Band H, Band V. Mammary epithelial cell transformation: insights from cell culture and mouse models. Breast Cancer Res 2005;7:171–9.
40. Cardiff RD, Anver MR, Gusterson BA, Hennighausen L, Jensen RA, Merino MJ, et al. The mammary pathology of genetically engineered mice: the consensus report and recommendations from the Annapolis meeting. Oncogene 2000;19: 968–88.
41. Liu BY, McDermott SP, Khwaja SS, Alexander CM. The transforming activity of Wnt effectors correlates with their ability to induce the accumulation of mammary progenitor cells. Proc Natl Acad Sci U S A 2004;101:4158–63.
42. Pirot F, Chaltiel D, Ben Lakhdar A, Mathieu MC, Rimareix F, Conversano A. Squamous cell carcinoma of the breast, are there two entities with distinct prognosis? A series of 39 patients. Breast Cancer Res Treat 2020;180:87–95.
43. Degnim AC, Visscher DW, Hoskin TL, Frost MH, Vierkant RA, Vachon CM, et al. Histologic findings in normal breast tissues: comparison to reduction mammaplasty and benign breast disease tissues. Breast Cancer Res Treat 2012; 133:169–77.
44. Teschendorff AE, Gao Y, Jones A, Ruebner M, Beckmann MW, Wachter DL, et al. DNA methylation outliers in normal breast tissue identify field defects that are enriched in cancer. Nat Commun 2016;7:10478.
45. Nakshatri H, Kumar B, Burney HN, Cox ML, Jacobsen M, Sandusky GE, et al. Genetic ancestry-dependent differences in breast cancer-induced field defects in the tumor-adjacent normal breast. Clin Cancer Res 2019;25:2848–59.
46. Ahuja D, Saenz-Robles MT, Pipas JM. SV40 large T antigen targets multiple cellular pathways to elicit cellular transformation. Oncogene 2005;24:7729–45.